

UNIVERSITI MALAYSIA PAHANG

BORANG PENGESAHAN STATUS TESIS ♦

JUDUL: PREDICTION OF GRINDING MACHINING PARAMETERS OF DUCTILE CAST IRON USING WATER BASED ZINC OXIDE NANOPARTICLE

SESI PENGAJIAN: 2011/2012

Saya, MOHD SABARUDIN BIN SULONG (890801-10-5871)

mengaku membenarkan tesis (Sarjana Muda / ~~Sarjana / Doktor Falsafah~~)* ini disimpan di perpustakaan dengan syarat-syarat kegunaan seperti berikut:

1. Tesis ini adalah hakmilik Universiti Malaysia Pahang (UMP).
2. Perpustakaan dibenarkan membuat salinan untuk tujuan pengajian sahaja.
3. Perpustakaan dibenarkan membuat salinan tesis ini sebagai bahan pertukaran antara institusi pengajian tinggi.
4. **Sila tandakan (√)

SULIT

(Mengandungi maklumat yang berdarjah keselamatan atau kepentingan Malaysia seperti yang termaktub di dalam AKTA RAHSIA RASMI 1972)

TERHAD

(Mengandungi maklumat TERHAD yang telah ditentukan oleh organisasi / badan di mana penyelidikan dijalankan)

TIDAK TERHAD

Disahkan oleh:

(TANDATANGAN PENULIS)

(TANDATANGAN PENYELIA)

Alamat Tetap:

Bt. 5, Kg. Kuantan
45000, Kuala Selangor
Selangor.

DR. MD. MUSTAFIZUR RAHMAN

Tarikh: 21 JUN 2012

Tarikh: 21 JUN 2012

CATATAN: * Potong yang tidak berkenaan.

** Jika tesis ini SULIT atau TERHAD, sila lampirkan surat daripada pihak berkuasa/organisasi berkenaan dengan menyatakan sekali tempoh tesis ini perlu dikelaskan sebagai SULIT atau TERHAD.

♦ Tesis dimaksudkan sebagai tesis bagi Ijazah Doktor Falsafah dan Sarjana secara Penyelidikan, atau disertasi bagi pengajian secara kerja kursus dan penyelidikan, atau Laporan Projek Sarjana Muda (PSM).

PREDICTION OF GRINDING MACHINING PARAMETERS OF DUCTILE CAST
IRON USING WATER BASED ZINC OXIDE NANOPARTICLE

MOHD SABARUDIN BIN HJ SULONG

Report submitted in partial fulfillment of requirements
for award of the Degree of
Bachelor of Mechanical Engineering

Faculty of Mechanical Engineering
UNIVERSITI MALAYSIA PAHANG

JUNE 2012

SUPERVISOR'S DECLARATION

I hereby declare that I have checked this report and in my opinion this report is satisfactory in terms of scope and quality for the award of the degree of Bachelor of Mechanical Engineering.

Signature:

Name: DR. MD. MUSTAFIZUR RAHMAN

Position: ASSOCIATE PROFESSOR

Date: 21st JUNE 2012

**UNIVERSITI MALAYSIA PAHANG
FACULTY OF MECHANICAL ENGINEERING**

I hereby declare that I have checked this project report and in my opinion this project is satisfactory in terms of scope and quality for the award of the degree of Bachelor of Mechanical Engineering.

Signature:

Examiner: DR. GIGIH PRIYANDOKO

Position: PENSYARAH KANAN

Date: 21ST JUNE 2012

STUDENT'S DECLARATION

I hereby declare that the work in this project report "*Prediction of Grinding Machining Parameter of Ductile Cast Iron using Water Based Zinc Oxide Nanoparticle*" is my own except for quotations and summaries which have been duly acknowledged. The report has not been accepted for any degree and is not contently submitted in candidate of any other degree.

Signature:

Name: MOHD SABARUDIN BIN HAJI SULONG

ID Number: MA 08050

Date: 21ST JUNE 2012

Dedicated to my beloved family and friends

ACKNOWLEDGEMENTS

I would like to show my highest gratitude to the almighty for blessing me in finishing the project. I am grateful and would like to express my sincere gratitude to my supervisor Associate Professor Dr. Md. Mustafizur Rahman his germinal ideas, invaluable guidance, continuous encouragement and constant support in making this research possible. He has always impressed me with his outstanding professional conduct, his strong conviction for science, and his belief that a program is only a start of a life-long learning experience. I appreciate his consistent support from the first day I applied to graduate program to these concluding moments. I am truly grateful for his progressive vision about my training in science, his tolerance of my naïve mistakes, and his commitment to my future career. I also sincerely thanks for the time spent proofreading and correcting my many mistakes.

My sincere thanks go to all my lab mates and members of the staff of the Mechanical Engineering Department, UMP, who helped me in many ways and made my stay at UMP pleasant and unforgettable. Many special thanks go to Grinding Laboratory assistant, Mr Aziha for his excellent co-operation, inspirations and supports during this study.

I acknowledge my sincere indebtedness and gratitude to my parents for their love, dream and sacrifice throughout my life. I offer my regards and blessings to all of those who supported me especially my family and friends in any respect during the completion of the project. All of their help are very significant to the success of this project. I cannot find the appropriate words that could properly describe my appreciation for their devotion, support and faith in my ability to attain my goals. Special thanks should be given to my committee members. I would like to acknowledge their comments and suggestions, which was crucial for the successful completion of this study.

ABSTRACT

This project presents the prediction the grinding machining parameters for ductile cast iron using water based Zinc Oxide (ZnO) nanoparticles as a coolant. Studies were made to investigate the experimental performance of ductile cast iron during grinding process based on design of experiment. Response surface modeling (RSM) is practical, economic and relatively easy for use. The experimental data was utilized to develop the mathematical model for first- and second order model by regression method. Contour plot is a helpful visualization of the surface when the factors are no more than three and in order to locate the optimum value. The quality of product was determined by output criteria that are minimum temperature rise, minimum surface roughness and maximum material removal rate. Based on prediction data, the second-order gives the good performance of the grinding machine with the significant p-value of analysis of variance that is below than 0.05 and support with R-square value nearly 0.99. From the model profiler and contour plot, the optimum parameter for grinding model is 20m/min table speed and 42.43 μ m depth of cut could for single pass grinding. For multiple pass grinding it optimized at the table of speed equal to 35.11m/min and 29.78 μ m depth of cut could for has best quality of product. As the conclusion, objectives were achieved where the grinding parameters were optimized, grinding performance was investigated and mathematical model for abrasive machining parameter was developed. The model was fit adequate and acceptable for sustainable grinding using 0.15% volume concentration of zinc oxide nanocoolant.

ABSTRAK

Projek ini membentangkan ramalan parameter pemesinan perlelasan bagi besi tuang mulur menggunakan Zink Oksida (ZnO) nanopartikel berasaskan air sebagai penyejuk. Kajian telah dibuat untuk menyiasat prestasi eksperimen besi tuang mulur semasa proses pelelasan berdasarkan reka bentuk eksperimen. Tindak balas pemodelan permukaan (RSM) adalah praktikal, ekonomi dan agak mudah untuk digunakan. Data eksperimen telah digunakan untuk membangunkan model matematik bagi model peringkat pertama dan kedua melalui kaedah regresi. Plot kontur adalah visualisasi membantu permukaan apabila faktor adalah tidak lebih daripada tiga dan untuk mencari nilai optimum. Kualiti produk telah ditentukan oleh kriteria output yang kenaikan suhu minimum, kekasaran permukaan minimum dan kadar penyingkiran bahan maksimum. Berdasarkan kepada data ramalan, peringkat kedua memberikan prestasi yang baik mesin pengisaran dengan ketara p-nilai analisis varians yang di bawah daripada 0.05 dan sokongan dengan nilai R-persegi hampir 0,99. Dari Profiler model dan plot kontur, parameter optimum bagi model pengisaran adalah 20m/min kelajuan meja dan kedalaman 42.43 μ m potongan boleh untuk pengisaran tunggal. Untuk pengisaran ulang-alik dioptimumkan di meja kelajuan yang sama dengan kedalaman 35.11m/min dan 29.78 μ m potongan mampu bagi mempunyai kualiti yang terbaik produk. Sebagai kesimpulan, objektif telah dicapai di mana parameter pengisaran dioptimumkan, prestasi pengisaran telah disiasat dan model matematik untuk parameter pemesinan melelas telah dibangunkan. Model itu patut mencukupi dan diterima untuk pengisaran mampan menggunakan jumlah kepekatan 0.15% daripada penyejuk nano zink oksida.

TABLE OF CONTENTS

		Page
SUPERVISOR’S DECLARATION		ii
EXAMINER DECLARATION		iii
STUDENT’S DECLARATION		iv
DEDICATION		v
ACKNOWLEDGEMENTS		vi
ABSTRACT		vii
ABSTRAK		viii
TABLE OF CONTENTS		ix
LIST OF TABLES		xii
LIST OF FIGURES		xiv
LIST OF SYMBOLS		xvi
LIST OF ABBREVIATIONS		xvii
CHAPTER 1 INTRODUCTION		
1.1	Introduction	1
1.2	Motivation of the Project	2
1.3	Objectives of Project	3
1.4	Scope of the Study	3
1.5	Organization of Study	3
CHAPTER 2 LITERATURE REVIEW		
2.1	Introduction	4
2.2	Types of Grinding	5
2.3	Machining Parameters	6
2.4	Nanofluids	10
	2.4.1 Cooling application	11
	2.4.2 Lubricant application	12

2.5	Nanofluids Preparation and Synthesis	13
2.5.1	Two-step physical process	13
2.5.2	One-step physical process	14
2.5.3	One-step chemical process	15
2.6	Thermal Conductivity	15
2.7	Statistical Method	16
2.7.1	First-order model	16
2.7.2	Second-order model	17

CHAPTER 3 EXPERIMENTAL DETAILS AND MODELLING

3.1	Introduction	19
3.2	Design of Experiments	19
3.3	Workpiece Preparation	21
3.4	Composition Analysis	24
3.5	Hardness Test	25
3.6	Nanocoolant Preparation	26
3.7	Grinding Process	29
3.8	Temperature Analysis	30
3.9	Surface Roughness Analysis	31
3.10	Scanning Electron Microscopy	32

CHAPTER 4 RESULTS AND DISCUSSION

4.1	Introduction	33
4.2	Material Removal Rate	33
4.3	Temperature Effect	41
4.4	Surface Roughness	48
4.5	Tool Wear	54
4.6	G-Ratio	56
4.7	Optimization	58
4.8	Scanning Electron Microscopic	60

LIST OF TABLES

Table No.	Title	Page
2.1	Thermal conductivity for various nanofluids	12
3.1	Design of experiment table	20
4.1	Material removal rate for each coolant and type of grinding	34
4.2	ANOVA for first order MRR prediction in single pass and multiple pass grinding using 0.15% volume concentration zinc oxide water based nanocoolant	36
4.3	ANOVA for second order MRR prediction in single pass and multiple pass grinding using 0.15% volume concentration zinc oxide water based nanocoolant	37
4.4	Differentiate between experimental value and prediction value of MRR.	39
4.5	Temperature rising	42
4.6	ANOVA for first order temperature rising in single pass and multiple pass grinding using 0.15% volume concentration zinc oxide water based nanocoolant	43
4.7	ANOVA for second order temperature rising in single pass and multiple pass grinding using 0.15% volume concentration zinc oxide water based nanocoolant	44
4.8	Experimental and predicted value from predicted temperature rising model	47
4.9	Surface finish for each coolant and type of grinding	49
4.10	ANOVA for first order surface roughness prediction in single pass and multiple pass grinding using 0.15% volume concentration zinc oxide water based nanocoolant	49
4.11	ANOVA for second order surface roughness prediction in single pass and multiple pass grinding using 0.15% volume concentration zinc oxide water based nanocoolant	50
4.12	Experimental and predicted value from predicted surface roughness model	52

4.13	Tool wear for each coolant and type of grinding	55
4.14	G-ratio for each coolant and type of grinding	57

LIST OF FIGURES

Figure No.	Title	Page
2.1	Type of grinding	5
2.2	G-ratio of various nanofluid coolant and different techniques	9
2.3	Variation of the thermal conductivity ratio of ZnO nanofluid with temperature	10
2.4	Nanoparticle size of zinc oxide	11
2.5	One-Step Physical Process	14
3.1	Cast iron ingots	21
3.2	Squaring process	23
3.3	3D Workpiece dimension and details view	23
3.4	Disc cutter.	24
3.5	Spark emission spectrometer	25
3.6	Brinell hardness test machine	26
3.7	Setup of mixture during dilution processes	28
3.8	Surface grinding machine	29
3.9	Clamp process	30
3.10	Calibration of table speed	30
3.11	Perthometer	31
3.12	Scanning electron microscope	32
4.1	Material removal rate for each coolant and type of grinding	35
4.2	Correlation of the second order model of MRR	38
4.3	Contour plot of the second order model of MRR	40

4.4	Relation between the experimental value and predicted value for both single pass grinding and multiple pass grinding	41
4.5	Correlation of the second order model of temperature rising	45
4.6	Contour plot (2D and 3D) of the second order model of temperature rising	46
4.7	Different between experimental values predicted value from predicted temperature rising model.	47
4.8	Correlation of the second order model of surface roughness	51
4.9	Contour plot of the second order model of surface roughness	53
4.10	Experimental and predicted value from predicted surface roughness model	54
4.11	Tool wears each coolant and type of grinding	56
4.12	G-ratio for each coolant and type of grinding	58
4.13	Prediction profiler for optimization in single pass grinding	59
4.14	Prediction profiler for optimization in multiple pass grinding	60
4.15	Scanning electron microscopic	61

LIST OF SYMBOLS

Mm	Millimetre
cm	centimetre
L	length
Ra	Roughness average
$W \cdot m^{-1} \cdot K^{-1}$	Watt per meter per Kelvin
m/min	Metre per minute
μm	micrometre
cm^3/min	Centimetre cubic per minute
L	Litter
CS	Cutting speed
A	Area
%	Percent
ϕ_1	Initial volume concentration
Ω	Weight percent of nanofluid
ρ_w	Density of water
ρ_{ZnO}	Density of zinc oxide particle
Δv	Volume of distilled water required
v_1	Initial volume of nanofluid before dilute

LIST OF ABBREVIATIONS

MRR	Material removal rate
ZnO	Zinc oxide
CuO	Cooper oxide
TiO	Titanium oxide
CLA	Center line average
Cu	Cooper
Fe	Ferrum
Au	Gold
Ag	Silver
SiC	Silicon carbide
Al ₂ O ₃	Aluminium oxide
SEM	Scanning electron microscope
TR	Temperature rising
SR	Surface roughness
MQL	Minimum quantity liquid
CuSO ₄ •5H ₂ O	Copper sulfate pentahydrate
NaH ₂ PO ₂ •H ₂ O	Sodium hypophosphite

CHAPTER 1

INTRODUCTION

1.1 INTRODUCTION

Grinding widely used as the finishing machine for components that require smooth surface roughness and precision dimension and the processes are mainly the technique employed widely as a finishing and difficult-to machine such as hardness and brittleness materials finishing. However, in the grinding process, high grinding zone temperature may lead to thermal damage to the work surface, induces micro-cracks and tensile residual stresses in the ground surfaces, which deteriorate since surface quality and integrality of the ground surface (Hryniewicz et al., 2001). On the other hand, wear on grinding wheel is also a major problem since grinding is an abrasive process where the two surfaces are sliding each other. To decrease the wear rate on grinding wheel is a great challenge. Thermal damage of the workpiece can reduce by the application of a flood delivery grinding fluid that removes the heat created by the workpiece interaction and lubricates the two surfaces in order to decrease the amount of friction and tool wear can be reduced (Brinksmeier and Minke, 1993)

Nanofluid is new class fluid engineered by dispersion of solid particle with small diameter measured in less than 100 nanometers in based fluid to enhance thermal properties and tribological properties. Nanofluids have the potential to be the next generation of coolants due to their significantly higher thermal conductivities. Appropriate selection of a base fluid is very critical in the application of nanoparticle-based lubricants in grinding and proper selection of the cutting parameters for machining is obtain performances (Hryniewicz et al., 2001). When there are suspended crystalline solid particle with nanometre dimension in the based fluid such as water,

ethylene glycol, lubrication oils, etc. to form a stable homogenous suspension and it increase the thermal conductivity relative to the based fluid so the suspension called Nanofluid. The thermal conductivity and the convection heat transfer coefficient of the fluid can be largely enhanced by the suspended nanoparticles (Malkin and Guo, 2007). Tribological research also found that lubricating oil with nanoparticle would exhibit the friction reduction properties. These features make nanofluid and nanoparticle useful and need to be improve beside apply in industries especially in heating and cooling, machining process, lubrication, transportation energy and electronics.

Response surface methodology (RSM) is combination of statistical technique where useful for analyzing and modelling problem in interested response that influence by several variables (Montgomery, 2005). The several experiment needs to conduct and the result from the experiment will collected before the data was analyzed. The goal of this research is an investigate maximum material removal rate and optimize machining parameter so that the surface roughness will minimize and material removal rate (MRR) to be maximized when using water based Zinc Oxide nanocoolant. Statistical method is used to prepare the design of experiments and find optimum parameters.

1.2 MOTIVATION OF THE PROJECT

Grinding is widely used in industries usually used as the finishing machining for components that require smooth surface roughness and precision dimension. It can produce very fine surfaces and very accurate dimensions and available in either hard or brittle materials. However, almost all energy in grinding process converts to heat and make the temperature rising up. The heat becomes concentrated in grinding zone so that the workpiece was heated at high temperature and possibility the workpiece surface damage due to the thermal effect (Komanduri and Reed, 2008). However, there is a little work on nanofluid based coolant in grinding processes since this is a new thing and lack of consistency result regarding thermal properties (Murshed et al., 2008; Wong and Kurma, 2008). There are a lot of previous research had done based on grinding process such as minimum quantity lubricant in the grinding process, surface modelling for conventional grinding, flow of the coolant etc. The goal of this research is coming

with prediction of material removal rate and optimum grinding characteristic of ductile cast iron using zinc oxide nano-particle.

1.3 OBJECTIVES OF PROJECT

The objectives of the project are as follows:

- i. To investigate the experimental performance of ductile cast iron during the grinding process based on design of experiment.
- ii. To develop mathematical models for abrasive machining parameter using response surface method.

1.4 SCOPE OF THE STUDY

- i. Design of experiment
- ii. Prepare ZnO nanocoolant.
- iii. Perform experiment on Grinding machine utilizing abrasive grinding wheel using water based ZnO nanocoolant on ductile cast Iron grinding process
- iv. Perform the statistical analysis using central composite methods and
- v. Perform surface roughness and G-ratio analysis

1.5 ORGANIZATION OF PROJECT

Chapter 2 presents the literature review on nanofluids, grinding process and response surface modelling. The methods of nanofluids synthesis were introduced, and their characteristic was discussed and for the grinding process, machining parameter involved such as wheel speed, table speed, depth of cut and other was discussed. Chapter 3 also presents the details information related to methodology of the experiment. Chapter 4 focuses on result and analysis, from the various combinations of input parameters such as wheel speed, table speed, depth of cut and G-ratio, material removal rate, surface roughness, and temperature. The results are analyzed to have an optimum input machining parameter. and the conclusions or recommendations for future work presented in Chapter 5.

CHAPTER 2

LITERATURE REVIEW

2.1 INTRODUCTION

Grinding is an abrasive process where the workpiece is a force against the grinding wheel. Because of abrasive wear, the process generates chips that remove from the workpiece surface. However, the forces that generate during the process are converted into heat that causing the high temperature, particularly at the wheel and the workpiece interfaces. Grinding is a large and diverse area of manufacturing and tool making. It can produce fine surfaces and very accurate dimensions and available in either hard or brittle materials. High temperatures can cause thermal damage to the workpiece, which affects the workpiece quality and limits the process productivity (Malkin and Guo, 2007). Grinding wheel wear is a major problem that needs to overcome. To control heat and wheel wear or to improve the grinding performance, a heavy amount of grinding fluids (coolant) is used. The conventional cutting fluids used in grinding are considered a problem, as these substances can cause a large amount of mist, which is environmentally challenging and is expensive (Silva et al., 2005). This research interested nanofluid as the coolant in grinding machining process.

Nanofluid is a new class of fluids engineered by dispersing nanometer-size solid particles in base fluids such as water, ethylene glycol, engine oil, cutting fluids. The thermal conductivity and the coefficient of convection heat transfer of the fluid can largely enhanced by the suspended nanoparticles recently. Tribology research shows that lubricating oils with nanoparticle additives. These features make the nanofluid very attractive in some cooling and/or lubricating application in many industries, including manufacturing, transportation, energy, and electronics. Previous study stated that

grinding conditions like depths of cut, work speed, wheel speed and others influence the surface roughness and hardening (Ramesh et al. 2004 and Gopal and Rao, 2003). Combinations of these input parameters are to investigate the relation to the surface roughness, temperature generates, material removal rate and G-ratio of the grinding wheel.

2.2 TYPE OF GRINDING

Grinding is most commonly used as a finishing process to achieve material removal and desired surface finish with acceptable surface integrity, dimensional tolerance and form tolerance. The tribological process, two dissimilar material surface contacts and sliding each other produce wear and abrasion on the surface, and the material is rapidly remove from the ground surface. There are many types of grinding such as belt grinder, bench grinder, cylindrical grinder, surface grinder and other. However, this research interested in the surface grinding machines because it was large used in industries.

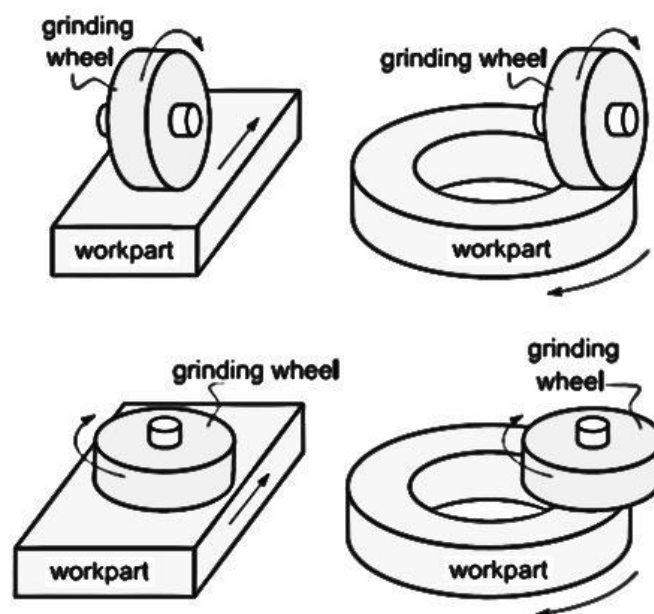


Figure 2.1: Type of grinding

Surface grinding is the most common operation for grinding flat surface and is likely to produce high tolerances, low surface roughness and planar surfaces. In surface

grinding, shallow depth of cut was achieved with fast feed rates and the depth of cut can range from 0.01 to 0.05mm while the feed rate is approximately 3m/s (Cameron et al., 2010). Figure 2.1 shows of surface grinding according to the workpiece shape and grinding wheel orientation. Surface grinders come up with lots of facilities. Precision surface grinders have absolutely vibration-free and noise-free operations. Some grinders have to provision for coolant applicants. In certain grinders, there are provisioned for gathering the dust particles, which is generated during the precision process.

2.3 MACHINING PARAMETERS

Grinding practice is a large and diverse area of manufacturing and tool making. It can produce fine surfaces and very accurate dimensions and available for either hard or brittle materials. Previous study stated that grinding conditioned like depths of cut, work speed, wheel speed, etc., influence the surface roughness and hardening. Several parameters involve in grinding machining process such as wheel speed, workpiece speed, depth of cut, type of grinding wheel, wheel grit, coolant flow, coolant concentration, type of coolant and other. However, in this research only interested in depth of cut, type of grinding wheel, type of coolant and finally yet importantly is table speed as their factor to overlook the response.

Depth of Cut: Surface grinding is the most common operation for grinding flat surface and is likely to produce high tolerances, low surface roughness and planar surfaces. In surface grinding, shallow depth of cut is achieved with fast feed rates and the depth of cut can range from 0.01 to 0.05mm (Cameron et al., 2010)

Workpiece Speed: During the surface grinding process, the work moves in two directions. As a flat workpiece is being ground, it moves under the grinding wheel from left to right (longitudinal traverse). This longitudinal speed is called work speed. The work also moves gradually from the front to rear (cross traverse), but this movement occurs at the end of each stroke and does not affect the work speed. The work moves from left to right (cross traverse) as the surface of the cylinder rotates under the grinding wheel (lateral traverse).

Grinding Wheel: There are a lot of grinding discs usually they have been specially coding to represent several data for ones grinding wheel. Cubic boron nitride grains have very high thermal conductivity, which can enhance heat conduction away from the grinding zone to the wheel (Upadhyaya and Malkin, 2004), and therefore, can prevent the thermal damage to the workpiece. Different grinding wheel manufacturers to slightly different methods for defining the specification of their own make of a wheel. They all generally follow the same type of format using a code made up of letters and numbers relating to different features within the wheel. Either this code is marked along the side of the grinding wheel, on the wheel blotter or if the wheels are too small, on an identification card which was sent with the grinding wheel.

Coolant: The cutting fluids used in grinding operations are the same as those used in other machine tool operations. Synthetic coolants are the best, but you also may use a mixture of soluble oil and water. As in most machining operations, the coolant helps to maintain a uniform temperature between the tool and the work to prevent extreme localized heating. Excessive heat will damage the edges of cutters, cause warpage, and may cause inaccurate measurements. In other machine tool operations, the chips fall aside and present no great problem. This embedding cause unsatisfactory grinding and need to dress the wheel frequently. A sufficient volume of cutting fluid helped prevent the loading. The fluid also helps to reduce friction between the wheel and the work and to produce a good finish. According to Verma et al. (2008), MoS_2 in its nanoparticulate form has exceptional tribological properties, which can reduce friction under extreme pressure conditions. Wu et al. (2006) examined the tribological properties of lubricating oils with CuO , TiO_2 , and diamond nanoparticles additives. The experimental results show that nanoparticles, especially CuO , added to standard oils exhibit good friction-reduction and anti-wear properties.

Surface Roughness: Surface roughness is variable used for describe the quality of ground surface as well as competitiveness of overall grinding system as it determines the quality of the workpiece characteristic such as the minimum tolerance, the lubricant effectiveness, and the component life (Hecker and Liang, 2003). When measurements of surface roughness are made, techniques based on statistics can be used to remove the effects of the reference surface (Wyant, 1985). The arithmetic average height

parameter (R_a), also known as the center line average (CLA), is mostly used as an index to determine the surface finish in the machining process. It defines as Eq. (2.1):

$$R_a = \frac{1}{l} \int_0^l [y(x)] dx \quad (2.1)$$

The roughness average, R_a is the most used international parameter of surface roughness. Surface roughness is the measure of the finer surface irregularities in the surface texture. It was quantified by the vertical deviations of a real surface from its ideal form. The surface is rough when the deviations are large while the surface is smooth when deviations are small and (Zhong and Venkatesh, 2008) a good-quality surface for the most industrial is with arithmetic mean roughness, R_a below $0.8\mu\text{m}$. Prediction and identification of surface roughness has been the subject of many researchers in the manufacturing field. From the literature, the modeling and prediction problems of surface roughness of a work-piece by mathematical modeling have received increasing attention.

Temperature: Grinding is tribological process where two dissimilar material surface contacts and sliding each other produce wear and abrasion of the surface, and the material is rapidly removed from the ground surface. Through this process, almost all energy converts to heat and make the temperature rising up. The heat becomes concentrated in grinding zone so that the workpiece will be heated at high temperature and possibility the workpiece damage by the thermal is increased. Temperature depends on a range of factors, including the type of coolant, method of coolant supply, type of grinding wheel and the speed and depth of cut. The heat generated in the process and plastic deformation in the surface layer of the part will produce a considerable amount of residual mechanical stress. (Guo et al., 2009). Temperature problems in scratching and grinding were, first studied in metal parts fabrication, in which a possible thermal burning may damage the tools and workpieces. The turning and grinding metals requires high input of energy per unit volume of material removal (Kohli et al., 1995), some of that heat is taken away by coolant, chips, workpiece and tool. The fraction of heat entering the workpiece is directly related to the temperature rise of the workpiece.

G-Ratio: Tool wear is normal in the machining process. However, there are many researches done to minimize this tool wear. G-ratio is the parameter that interested to analyze the tool wear. The grinding wheel wear occurs due to the friction between the abrasive grains and the workpiece. High fluid lubricating capacity reduces the wear on the grinding wheel by decreasing grain-workpiece friction, allowing the abrasive grains to remain bound to the binder for longer periods and leading to lower wear of the tool (Silva et al., 2005). G-ratio is accepted a parameter of wheel wear in the grinding ratio. It defines as Eq. (2.2):

$$G = \frac{\text{volume of material removed}}{\text{volume of wheel wear}} \quad (2.2)$$

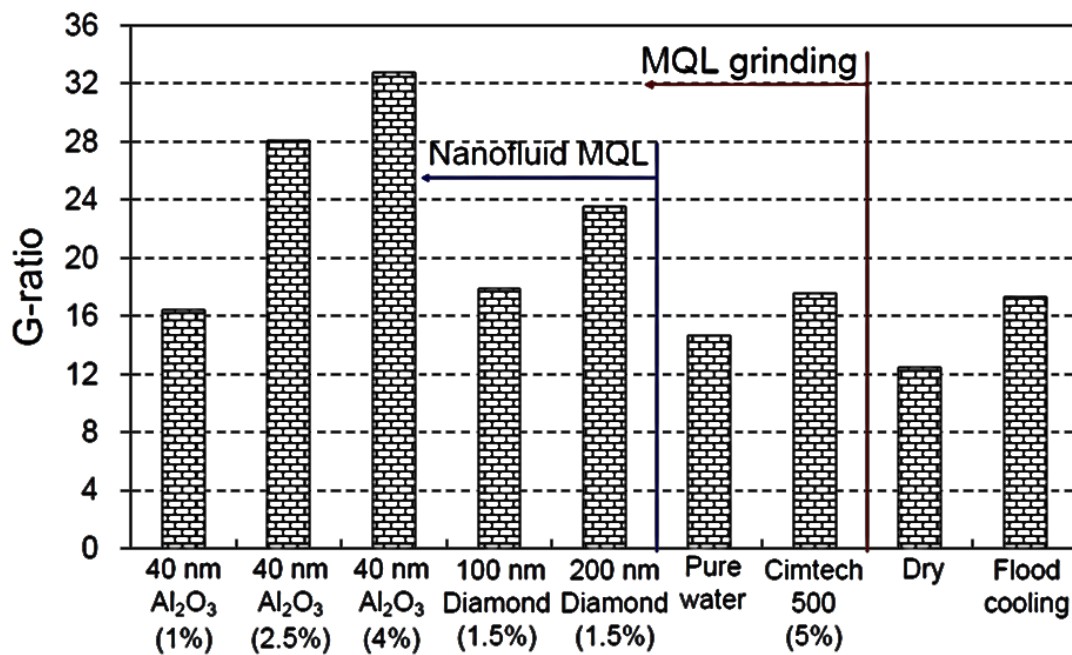


Figure 2.2: G-ratio of various nanofluid coolant and different techniques

Figure 2.2 shows the experimental results of the G - ratio, which is defined as the volume of material removed per unit volume of grinding wheel wear, could be improve with high concentration nanofluids. A high G-ratio indicates low wheel wear rate (Shen et al., 2008). In early research; it was found that a thin slurry layer of silicon carbide on the wheel surface could protect the bonding material from thermal and/or mechanical degradation or damage, thereby causing a high G-ratio (Komanduri and Reed, 1980).

2.4 NANO FLUIDS

Nanofluids generally classified into two categories, which is metallic nanofluids and non-metallic nanofluids (Eastman et al., 2004). Metallic nanofluids often refer to those containing metallic nanoparticles such as copper (Cu), ferrum (Fe), gold (Au) and silver (Ag), while nanofluids containing non-metallic nanoparticles such as aluminum oxide (Al₂O₃), copper oxide (CuO) and silicon carbide (SiC) are often considered as nonmetallic nanofluids. The measured thermal conductivity of the nanofluids containing 10, 30, and 60 nm-sized ZnO particles are 0.637, 0.627, and 0.618 W·m⁻¹·K⁻¹ at 20 °C, respectively, at a volume fraction of 1 % while that of pure water is 0.607 W·m⁻¹·K⁻¹. Note that the thermal conductivity of ZnO is 29 W·m⁻¹·K⁻¹ at 46 °C. The enhancement ratio relative to pure water is therefore 1.8~4.9 %. The enhancement ratio increases with the volume fraction and reaches 7.3~14.2 % at 3 % volume fraction. The measured thermal conductivity of the nanofluid is inversely proportional to the mean size of the suspended particles at a fixed volume fraction, suggesting that the laser fragmentation process can increase the thermal conductivity. Variation of the thermal conductivity ratio of ZnO nanofluid with temperature is shown in Figure 2.3. As observed earlier, the thermal conductivity ratio increases with an increase in temperature as well as particle volumetric concentration (Vajjha and. Das, 2009).

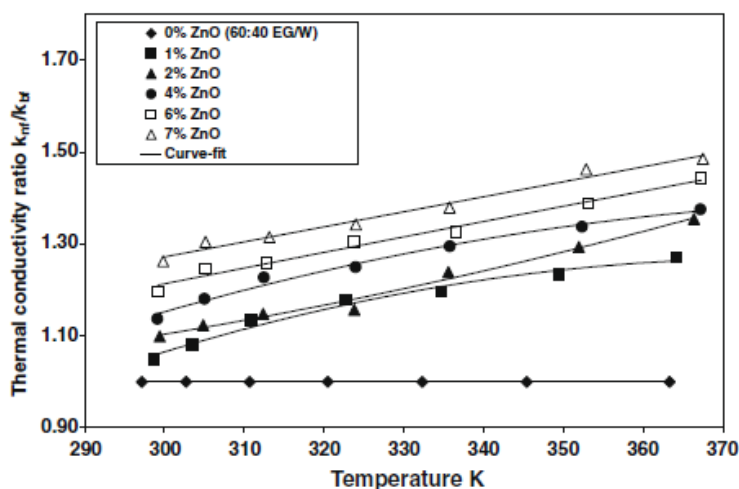


Figure 2.3: Variation of the thermal conductivity ratio of ZnO nanofluid with temperature

There has not been a systematic experimental investigation of size-dependent conductivity reported (Jang and Choi, 2004). However, Wang et al. (1999) compared their experimental data with those of other investigators, and concluded that it is possible that the thermal conductivity of nanoparticle fluid mixtures increases with the decreasing particle size. How the particle size affects the thermal conductivity of nanofluids will be studied in this research. Figure 2.4 shows the nanoparticle size of zinc oxide (Shen et al., 2008).

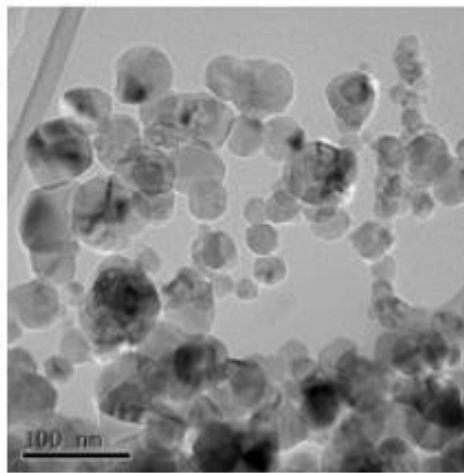


Figure 2.4: Nanoparticle size of zinc oxide

2.4.1 Cooling Applications

Nanofluid can enhance thermal conductivity that affects the heat transfer rate. Thermal conductivity also goes up with fraction of nano-particle. However, there is a little information on nanofluid as a coolant since this is new thing and the result from the research that had done come with lack of consistency result regarding thermal properties (Murshed et al., 2008, Wong and Kurma, 2008). Nanofluid had been using for cooling application in industries such as in nuclear reactor, transportation, automotive application, electronic and lubrication (Yu et al., 2008). Phase change nanoparticle in nanofluid simultaneously enhances the effective thermal conductivity and specific heat of the fluids. This leads to similar studies allow industrial cooling applications to continue without thorough understanding of all the heat transfer mechanisms in nanofluids (Han et al., 2008). High thermal conductivity in nanofluid that resulted from add the nanopartilce really benefit the conventional fluid like engine

oils, automatic transmission fluids, coolants, lubricants, and other synthetic high temperature heat transfer fluids usually found in conventional transportation such as car, truck radiators, engines, heating, ventilation and air-conditioning (HVAC) which known inherently have poor thermal properties (Yu et al., 2008; Chopkar et al., 2006). The application of nanofluid also contributed to a reduction of friction and wear, reducing parasitic losses, operation of components such as pumps and compressors, and subsequently leading to more than 6% fuel savings. When using high-thermal conductive nanofluids in radiators, it can lead to a reduction in the frontal area of the radiator by up to 10%. This reduction in aerodynamic drag can lead to a fuel savings of up to 5%. Table 2.1 is listed the thermal conductivity of various nanofluids (Singh et al., 2006).

Table 2.1: Thermal conductivity for various nanofluids.

Material	Thermal conductivity (w/m-K) @ 300K
Metallic solid	
Copper	401
Aluminum	237
Titanium	22
Nonmetallic solids	
Diamond	2300
Silicon	148
Aluminum Oxide	36
Conventional heat transfer fluid	
Water	0.613
Ethylene Glycol	0.252
Engine Oil	0.145

2.4.2 Lubrication Applications

To improve the tribological properties of lubricating oils by dispersing nanoparticles, especially nanoparticulate solid lubricants, becomes of interest to societies. Research has shown that lubricating oils with nanoparticle additive's exhibit improved load-carrying capacity, anti-wear and friction-reduction properties. (Xu et al., 1996) investigated tribological properties of the two-phase lubricant of paraffin oil and diamond nanoparticles, and the results showed that, under boundary lubricating conditions; this kind of two-phase lubricant possesses excellent load-carrying capacity, anti-wear and friction-reduction properties. According to (Verma et al. 2007), MoS₂ in

its nanoparticulate form has exceptional tribological properties, which can reduce friction under extreme pressure conditions. Wu et al. (2006) examined the tribological properties of lubricating oils with CuO, TiO₂, and diamond nanoparticles additives. The experimental results show that nanoparticles, especially CuO, added to standard oils exhibit good friction-reduction and anti-wear properties.

2.5 NANOFUIDS PREPERATION AND SYNTHESIS

The first problem need to solve is stability to prepare nanofluid. Stability of nanofluid divides to three aspects, which is kinetic stability where nanoparticles dispersed in the nanofluids has strong Brownian movements. The mobility of the nanoparticles can offset their sedimentation caused by the gravity field. In other hands, dispersion stability is due to the aggregation of nanoparticles; the dispersion of nanoparticles in fluids may deteriorate with time. Finally, chemical stability where no chemical reactions either between the suspended nanoparticles or between the base fluid and nanoparticles are desired at the working conditions of the nanofluids. The last stability can be realized by choosing the right nanoparticles and fluids according to the working environment.

2.5.1 Two-steps Physical Process

Nanoparticles are first produced as a dry powder, typically by inert gas–condensation, which involves the vaporization of a source material in a vacuum chamber and subsequent condensation of the vapor into nanoparticles via collisions with a controlled pressure of an inert gas such as helium. The resulting nanoparticles are then dispersed into a fluid in a second processing step. An advantage of this technique in terms of eventual commercialization of nanofluids is that the inert-gas condensation technique has already been scaled up to economically produce tonnage quantities of nano powders (Wagener and Gunther, 1999).

2.5.2 One-Step Physical Process

This technique synthesizes nanoparticles and disperses them into a fluid in a single step. It was originally used to prepare extremely fine particles of Ag by vacuum evaporation onto a running oil substrate, which was developed by Yatsuya et al. (1978) and later improved by Wagener and Gunther (1999). This technology is to produce nanofluids. As shown in Figure 2.5 the technique involves vaporization of a source material under vacuum conditions, and condensation from the vapor occurs via contact between the vapor and a flowing liquid. Nanoparticle agglomeration is minimized by flowing the liquid continuously, which results in the good dispersion. However, the one-step physical process is very expensive and at present the volume of nanofluids that can be produced via this direct-evaporation technique is much more limited than with the two-step physical process because of the limited space inside the vacuum chamber (Eastman et al., 1997)

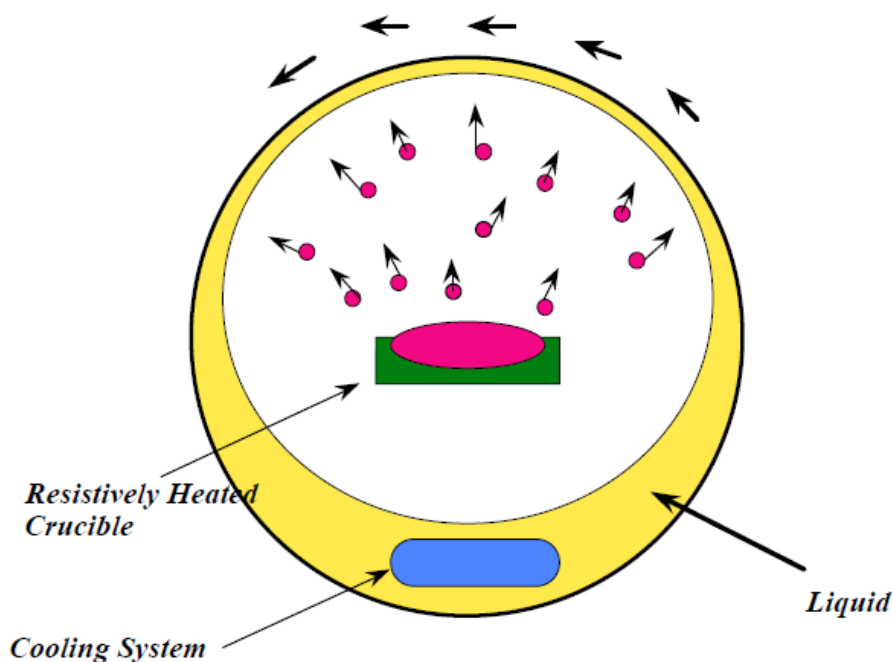


Figure 2.5: One-Step Physical Process

Source: (Shen et al., 2008).

2.5.3 One-step Chemical Process

To develop a one-step chemical process for producing stable Cu in ethylene glycol nanofluids by reducing copper sulfate pentahydrate ($\text{CuSO}_4 \cdot 5\text{H}_2\text{O}$) with sodium hypophosphite ($\text{NaH}_2\text{PO}_2 \cdot \text{H}_2\text{O}$) in ethylene glycol under microwave irradiation. The thermal conductivity enhancement approaches that of the Cu nanofluids prepared by a one-step physical method. It is found to be a fast, efficient one-step chemical method to prepare Cu nanofluids. However, this method is still in the research stage and the types of nanofluid sit can produce are limited. Thus, we will not use one step chemical process to produce nanofluids in our research (Zhu et al., 2004).

2.6 THERMAL CONDUCTIVITY

Since thermal conductivity is the most important parameter responsible for enhanced heat transfer, many experimental works had been reported on this, the steady-state parallel-plate technique (Wang et al, 1999) and the temperature oscillation technique has been employed to measure the thermal conductivity of nanofluids (Das et al., 2003). Among these, the transient hot wire method has been used most extensively. Because in general, nanofluid sare electrically conductive, it is difficult to apply the ordinary transient hot-wire technique directly. A modified hot-wire cell and electrical system were proposed by coating the hot wire with an epoxy adhesive which have excellent electrical insulation and heat conduction (Nagasaka and Nagashima,1981).

However, Das et al. (2003) pointed out that possible concentration of ions of the conducting fluids around the hot wire might affect the accuracy of such experimental results. Xie et al. (2007) prepared and measured the thermal conductivities of 26 nm and 0.6 μm SiC suspensions in deionized water and EG using a transient hot-wire method. Different from experimental results of Lee at al. (1999), they found that the nanofluids with the same solid particles in different base fluids had the same improvement in the effective thermal conductivity.

2.7 STATISTICAL METHOD

Response surface methodology (RSM) is popular where it usefully applied in many manufacturing situations. In response surface methodology, the factors that are consider as most important are used to build a polynomial model in which the independent variable is the experiment's response. In addition, analytical models that are developed by using conventional approaches such as the statistical regression technique, which is combined with the RSM have remained as an alternative in the modeling of the machining process. RSM is practical, economical and relatively easy for use. The experimental data were utilized to build mathematical model for first- and second order model by regression method (Sahin and Motorcu, 2005). RSM are designs and models for working with continuous treatments when finding the optimal or describing the response is the goal (Oehlert 2000). The first goal for RSM is to find the optimum response. When there is more than one response then it is important to find the compromise optimum that does not optimize only one response (Oehlert 2000). To provide some context, there is good commercial software available to help with designing and analyzing response-surface experiments. One of the important facts is whether the system contains a maximum or minimum or a saddle point, which has a wide interest in the industry. Therefore, RSM is increasingly used in the industry. In addition, in recent years more emphasis has been placed by the chemical and processing field for finding regions where there is an improvement in response instead of finding the optimum response (Myers et al., 1989). In result, application and development of RSM will continue to be used in many areas in the future.

2.7.1 First-Order Model

Bradly (2007) stated that when the response can define by a linear function of independent variables, then the approximating function is a first-order model. A first-order model with two independent variables can be express as Eq. (2.2):

$$y = \beta_o + \beta_1x_1 + \beta_2x_2 + \varepsilon \quad (2.2)$$

First-order model is used to describe the flat surfaces that may or may not be tilted. This model is not suitable for analyzing maximum, minimum, and ridge lines. First-order model assumed an adequate approximation of true surface in a small region of the x 's (Montgomery, 2005). A first-order model uses low-order polynomial terms to describe some part of the response surface (Bradly, 2007). This model is appropriate for describing a flat surface with or without tilting surfaces. Usually a first-order model fits the data by least squares. Once the estimated equation is obtained, an experimenter can examine the normal plot, the main effects, the contour plot, and ANOVA statistics (F -test, t -test, R^2 , the adjusted R^2 , and lack of fit) to determine adequacy of the fitted model. Lack of fit of the first-order model happens when the response surface is not a plane. When there is a significant lack of fit of the first-order model, then a more highly structured model, such as the second-order model, may be studied in order to locate the optimum.

2.7.2 Second-Order Model

When there is a curvature in the response surface, then a higher degree polynomial to be used. The approximating function with two variables is calling a second-order model, and the equation is as Eq. (2.3):

$$y = \beta_0 + \beta_1x_1 + \beta_2x_2 + \beta_{11}x_{11}^2 + \beta_{22}x_{22}^2 + \beta_{12}x_1x_2 + \varepsilon \quad (2.3)$$

When there is a curvature in the response surface, the first-order model is insufficient. A second-order model is useful in approximating a portion of the true response surface with parabolic curvature. The second-order model includes all the terms in the first-order model, plus all quadratic terms like the second-order model is flexible, because it can take a variety of functional forms and approximates the response surface locally. Therefore, this model is usually a good estimation of the true response surface (Bradly, 2007). Second-order model describes quadratic surfaces, and this kind of surface can take many shapes. Accordingly, response surface can represent maximum, minimum, ridge or saddle point. Contour plot is a helpful visualization of the surface when the factors are no more than three. When there are more than three design variables, it is almost impossible to visualize the surface. For that reason, in order to

locate the optimum value, one can find the stationary point. Once the stationary point is located, an experimenter can either draw a conclusion about the result or continue in further studying of the surface.

CHAPTER 3

EXPERIMENTAL DETAILS AND MODELLING

3.1 INTRODUCTION

This chapter discussed about the overall work flow progress on the project that mainly to investigate the performance of ductile cast iron during grinding process based on design of experiment and develop the mathematical model for abrasive machining parameter using RSM. In general, it is used design of experiment (DOE) method for the experiment. A DOE is techniques enables designers to determine simultaneously the individual and interactive effects of many factors that could affect the output results in any design. The mathematical model is developed using the response surface method based upon experimental data. The preparation of workpiece and nanofluids are also discussed throughout this chapter. Several of combination of grinding parameter such as depth of cut, type of grinding wheel and direction of the grinding, the experiment was conducted and collected data. The data will be analyzed using RSM method was to determine the best response such as surface roughness, temperature generated during grinding, material removal rate and G-ratio.

3.2 DESIGN OF EXPERIMENTS

Design of experiments techniques enables designers to determine simultaneously the individual and interactive effects of many factors that could affect the output results. In the later stages of the experimental work, the goal shifts from screening to product and process optimization. The statistical experimental designs most widely used in optimization experiments are termed "response surface designs." In addition to trials at the extreme level settings of the variables, response surface designs contain trials in

which one or more of the variables are set at the midpoint of the study range. Thus, these designs provide information on direct effects, pair wise interaction effects and curvilinear variable effects. However, the central composite design (CCD) is the most popular of the many classes of RSM designs due to the following three properties:

A CCD can run sequentially. It can be naturally partitioned into two subsets of points; the first subset estimates linear and two-factor interaction effects while the second subset estimates curvature effects. The second subset need not be run when analysis of the data from the first subset points indicates the absence of significant curvature effects. CCDs also are very efficient, providing much information on experiment variable effects and overall experimental error in a minimum number of required runs. It is very flexible. There is good commercial software available to help with designing and analyzing response-surface experiments. Table 3.1 shows the DOE table that generates using SAS JMP 10.0 software. Experiment was conducted based on DOE table and different types of coolant. Zinc oxide (ZnO) nanocoolant with 0.15% volume concentration and conventional coolant is soluble oil water based coolant using constant grinding wheels, which is vitrified bond aluminum oxide grinding wheel (PSA-60JBV).

Table 3.1: Design of experiment table

Specimen	Table speed (m/min)	Depth of cut (μm)	Temperature different ($^{\circ}\text{C}$)	Material Removal Rate (cm^3/min)	Surface Roughness (μm)
A	20	20	-	-	-
B	20	40	-	-	-
C	20	60	-	-	-
D	30	20	-	-	-
E	30	40	-	-	-
F	30	60	-	-	-
G	40	20	-	-	-
H	40	40	-	-	-
I	40	60	-	-	-

In this project, the parameters that consider are depth of cut that has three levels 20 μ m, 40 μ m and 60 μ m. Second parameter is table speed also set at three levels 20m/min, 30m/min and 40m/min. There are other two categorical factors, which is type of coolant and grinding pass. Zinc Oxide nanofluid with 0.15% volume concentration and 5% volume concentration conventional water based soluble oil are choosing as a coolant. On the other hand, there are two types of grinding considered, which are single pass, and multiple pass set to 10 passes.

3.3 WORKPIECE PREPARATION

Figure 3.1 shows the ductile cast iron ingots that were machined using carbide cutting tool in the dry end milling condition. Milling is the most common form of machining, a material removal process, which can create a variety of features on a part by cutting away the unwanted material. The milling process requires a milling machine, workpiece, fixture, and cutter. The workpiece is a piece of pre-shaped material that is secured to the fixture, which itself is attached to a platform inside the milling machine. The cutter is a cutting tool with sharp teeth that was secured in the milling machine and rotates at high speeds. By feeding the workpiece into the rotating cutter, material is cut away from this workpiece in the form of small chips to create the desired shape. Milling is typically use to produce parts that are not axially symmetric and have many features, such as holes, slots, pockets, and even three-dimensional surface contours.



Figure 3.1: Cast Iron Ingots

Parts that are fabricated completely through milling often include components that are used in limited quantities, perhaps for prototypes, such as custom designed fasteners or brackets. Due to the high tolerances and surface finishes that milling can offer, it is ideal for adding precision features to a part whose basic shape had already been formed. In milling, the speed and motion of the cutting tool was specified through several parameters. These parameters are selected for each operation based upon the workpiece material, tool material, tool size, and more. Spindle speed is determined by Eq. (3.1):

$$spindlespeed = \frac{CS \times 100}{\pi d} \quad (3.1)$$

Where CS is cutting speed and d is cutter diameter.

Machining problems associated with cast iron were drilling, milling, turning and other machining processes. Most of the problems were due to the microstructure formation/changes during the machining process. During the high pressure drilling operation, the matrix structure of the cast iron was changed actually due to stress transformation of the high carbon-retained austenite in the matrix into martensite (Griffin et al., 2007). Milling process had done using Partner milling machine with digital panel show the distance travel. The spindle speed was calculated and set constantly and the feed rate was set by automatically. As a result, a long square block of cast iron was prepared. As illustrate in Figure 3.2, the ingot was clamp at the table of the milling machine and the squaring process had done to a small block.

From the square block, it is cut into smaller part as illustrate in Figure 3.3. The dimension of the workpiece is 65 mm × 30mm × 20mm. This process is done using band saw machine (Everising S-300 HB) with flood coolant. It takes time, however, the surface roughness quit fine. The coolant cools down the workpiece to ensure there are no burn and make the tool life more last lasting.



Figure 3.2: Squaring process

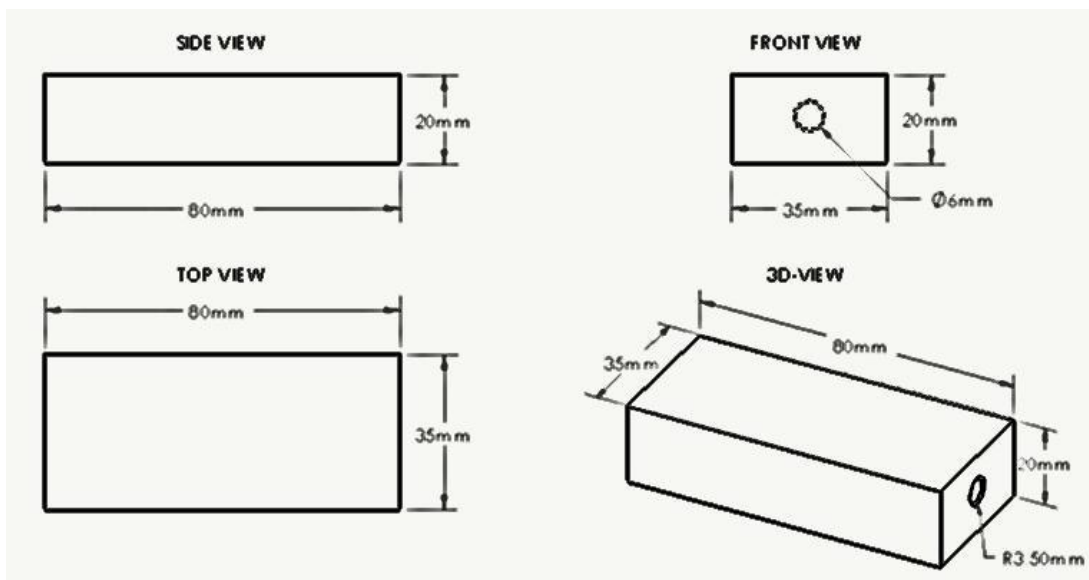


Figure 3.3: 3D Workpiece dimension and details view

3.4 COMPOSITION ANALYSIS

Firstly the ingots was cut using disk cutter as illustrate in Figure 3.4, since it is two flat surface after the cutting process the surface was polish using portable grinder until the surface are flat enough and smooth. The thickness of the plate is about 2.00 cm. Spark emission spectrometer was used to determine the composition of the metal to ensure that the ingot is cast iron. Before undergo the testing composition analysis process, the surface of the surface grinding must be flat enough. Therefore, the ingot was cut into a slice using disc cutter as illustrate. After get a vertical slice form the ingot the specimen had undergo grinding process to have a flat and smooth surface. Only smooth and flat surface only guide to consistence result. Appendix A shows the results of composition of cast iron.



Figure 3.4: Disc cutter

The main objective of this composition analysis is to ensure that the ingot was ductile cast iron Ductile cast iron round bars were prepared, usually using alloys with carbon equivalent percentage (C.E) ranging between 4.50 % and 4.76 %. Different measurements were carried out on as – cast and heat-treated specimens. Ductile cast

iron is essentially a family of materials with a wide variety of properties which are satisfactory for different engineering requirements. The soft ferrite grades are available to use when toughness and ductility are needed, while the harder pearlitic grades are used when higher strength is required. Grades with mixture of pearlite and ferrite in the matrix are also available. In addition, heat treatments of the previous types present different and better combination of properties for application with special requirements.



Figure 3.5: Spark emission spectrometer

3.5 HARDNESS TEST

Hardness of materials has probably been assessed by resistance to scratching or cutting. An example would be material B scratches material C, but not material A. Alternatively, material. The usual method to achieve a hardness value is to measure the depth or area of an indentation left by an indenter of a specific shape, with a specific force applied for a specific time. There are three principal standard test methods for expressing the relationship between hardness and the size of the impression, these being Brinell, Vickers, and Rockwell. For practical and calibration reasons, each of these methods is divided into a range of scales, defined by a combination of applied load and indenter geometry. The Rockwell scale is the most widely employed hardness scale. Rockwell gives increased exposure of the indentation hardness of a sample. It is able to

identify the hardness of the material employing a Rockwell hardness tester by measuring the precise depth of penetration of the indenter. The result of the test is indicated through a dimensionless number. The hardness of any sample basically correlates with its tensile strength. Due to the fact of this, it's also probable to test fantastic loads of samples employing portable testers. Rockwell hardness tester is also commonly use in the inspection to cast iron. All the parts with smaller grains, if there is not enough space for the Brinell hardness test, can be tested by Rockwell hardness tester. For pearlitic malleable iron, chilled cast iron and steel castings, HRB or HRC scale can be use, and if the material is heterogeneous, several readings should be measure to get the average value. Rockwell hardness testis quick, convenient and has small indentation, which can be use to directly test the finished piece. It is suitable for testing mass production of finished or semi-finished parts piece by piece (Figure 3.6).



Figure 3.6: Brinell hardness test machine

3.6 NANOCOOLANT PREPARATION

In this research, two step method was use to prepare nanaofluid, basically nanoparticles are first produced as a dry powder, typically by inert gas–condensation, which involves the vaporization of a source material in a vacuum chamber and subsequent condensation of the vapor into nanoparticles via collisions with a controlled

pressure of an inert gas such as helium. The resulting nanoparticles are then dispersed into a fluid in a second processing step. An advantage of this technique in terms of eventual commercialization of nanofluids is that the inert-gas condensation technique has already been scaled up to economically produce tonnage quantities of nanopowders. Thus, the dispersed nanoparticle come in liquid form with volume of one liter have 20% weight concentration with 30-40 nm particle size with 8.9 pH level and density equal to 5600kg/m³. From this data, it is diluted to be 0.15% volume concentration. The conversion of weight percent concentration to volume concentration expressed by Eq. (3.1). The second equation shows the dilution formula to determine how much distills water required to dilute the initial nanofluid.

$$\phi_1 = \frac{\omega \rho_w}{\frac{\omega}{100} \rho_w + (1 - \frac{\omega}{100}) \rho_{ZnO}} \quad (3.2)$$

Where

ϕ_1 = initial volume concentration

ω = weighth percent of nanoparticle

ρ_w = density of water

ρ_{ZnO} = density of nanoparticle

Thus

$$\phi_1 = \frac{(20)(100)}{\frac{20}{100}(1000) + (1 - \frac{20}{100})5600} \quad (3.3)$$

Volume concentration is $\phi_1 = 4.27$

$$\Delta v = v_1 \left(\frac{\phi_1}{\phi_2} - 1 \right) \quad (3.4)$$

Where, Δv = volume of distill water required;

v_1 = initial volume of nanofluid before dilution;

ϕ_1 = initial volume concentration;

ϕ_2 = final volume concentration

So: $16.5 = v_1 \left(\frac{4.27}{0.15} - 1 \right)$

$v_1 = 600mL$

As a result, to dilute Zinc Oxide nanofluid with initial volume concentration equal to 4.27% to low concentration Zinc Oxide nanofluid with final volume concentration equal to 0.15% required initial volume of nanofluid equal to 600mL dilute in 16.5 L distilled water. For a two-phase system, there are some important issues that have to face. One of the most important issues is the stability of nanofluids, and it remains a big challenge to achieve the desired stability of nanofluids. To achieve stability in dilution, one hour required to stir the solution continuously with the mixture set to 1000 rpm. Figure 3.7 shows the setup of mixture during dilution processes. Nanoparticles have the tendency to aggregate. The important technique to enhance the stability of nanoparticles in fluids is the use of surfactants. However, the functionality of the surfactants under high temperature is also a big concern, especially for high-temperature applications. Therefore, the surfactant is not applied in this project.



Figure 3.7: Setup of mixture during dilution processes

3.7 GRINDING PROCESS

The grinding process was done using Supertec precision grinding machine, model STP-102ADCII. The setup of the grinding experiment is shown in Figure 3.8. A vitrified bond aluminum oxide grinding wheel (PSA-60JBV) with 60-grain size average abrasive size was used. The workpiece material was block ductile iron with a carbon content of 3.5-3.9% and average hardness of 110- Rockwell C. The width and length of the workpiece surface for grinding are 35 mm and 80 mm, respectively.



Figure 3.8: Surface grinding machine

It starts with clamp the workpiece on a clamper jaw since cast iron will not attract to magnet field. Then find the zero point of Z-axis where the grinding disc is down slowly until there are some sparks. After that, coolant is spray directly to the workpiece to ensure the temperature of the workpiece equivalent to the temperature of the coolant and as precaution to get exact value of temperature rising. Figure 3.9 shows the clamping process. Next process is calibration of workpiece speed using tachometer. Figure 3.10 shows the calibration of table speed of Supertec precision grinding machine. The model STP-102ADCII can be control and using hydraulic system to move left and right. The speed are control by a control valve however there are no display for the speed, so that in this research calibration of the table speed using tachometer had done to measure and set the speed to be 20 mm/min, 30 mm/min and 40 mm/min.



Figure 3.9: Clamp process



Figure 3.10: Calibration of table speed

3.8 TEMPERATURE ANALYSIS

A grinding wheel can be considered as a carrier of massive grains, which act as abrading heat sources. Therefore, in the study of the grinding process cutting forces, heat generation and temperature rise must be taken into consideration. Generally, white cast iron is hard and brittle, which is difficult to machine. In addition, the casting process is never perfect especially when dealing with large components (Gonzalez and Mackay, 2001). While grinding, it is quite a challenge to take the reading of the temperature so the best device to measure the temperature is a thermocouple. A thermocouple is an electrical device that responds to a difference in temperature by producing an electric current. Thermocouples are used as measuring instruments and as control devices. Thermocouples are simple and rugged, can be used over a wide range

of temperatures (from -200°C . to 1600°C .). In this research K-type thermocouple was used, one hole had drilled in the center of the workpiece with the diameter just fit with the sensor.

3.9 SURFACE ROUGHNESS ANALYSIS

Surface finish must be controlled for increasing the fatigue strength of highly stressed members, which are subjected to load reversals. A smooth surface eliminates the sharp irregularities, which are the greatest potential source of fatigue cracks. For parts such as gears, surface finish control may be necessary to ensure quiet operations. In other cases, however, where a boundary lubrication condition exists or where surfaces may not be compatible, as in two extremely hard surfaces running together, a slightly roughened surface will usually assist in lubrication. A specific degree of surface roughness is also required in order to accommodate wear-in of certain parts. Most new moving parts do not attain a condition of complete lubrication because of imperfect geometry, running clearances, and thermal distortions. Therefore, the surfaces must wear in by a process of actual removal of metal. The surface finish must be a compromise between sufficient roughness for proper wear-in and sufficient smoothness for expected service life. In this research, Perthometer illustrated in Figure 3.11, three reading are taken and averages are calculated and both directions either follow the grinding direction or cross the direction of grinding.



Figure 3.11: Perthometer

3.10 SCANNING ELECTRON MICROSCOPY

Figure 3.12 shows the scanning electron microscope machine. Scanning electron microscopy (SEM) was carried in order to study the surface topography of the workpiece in result to the grinding process using two different coolants. It was done to ensure the effect of type of coolant on surface grinding either 5% volume concentration of soluble oil coolant or 0.15% volume concentration of zinc oxide nanocoolant is better.



Figure 3.12: Scanning electron microscope

CHAPTER 4

RESULTS AND DISCUSSION

4.1 INTRODUCTION

This chapter presents with the results obtained from mathematical modelling of the performance characteristics of grinding of ductile cast iron with zinc oxide nanofluids as a coolant. The mathematical models used for prediction of material removal rate, surface roughness, and tool wear rate are presented in this chapter. These models are developed using the accumulated data obtained from experimentation with between conventional soluble oil coolant and zinc oxide (ZnO) nanocoolant. The significance and adequacy of these models are verified by analysis of variance using the response surface method.

4.2 MATERIAL REMOVAL RATE

Material removal rate is rate of the material remove per unit time. The unit of material removal rate is centimetre cubic per second (cm^3/s), the mass reduce was measured using digital mass balance. Two reading were taken which is initial mass and final mass. Initial mass is the mass workpiece before the grinding process started and final mass is the mass of workpiece after the grinding process had finish and the reading was take after the mass balance reach the steady state. Hence, the material is removed by the action of abrasive process between the grinding wheel and the workpiece to find the optimum material removal rate. Based on the analysis of variance (ANOVA) all four factors were investigate either influent the material removal rate (MRR) and most significant factor for of MRR was investigate. Material removal rate for conventional and nanocoolant and single and multi-pass grinding processes are represented in

Table 4.1. The experiment had conduct nine times with various combination of table speed and depth of cut. Coolant apply in this setup is water based with 5% of volume concentration of soluble oil coolant and 0.15% volume concentration zinc oxide nanocoolant. It can be observed that the minimum material removal rate in single pass grinding using 5% volume concentration of conventional coolant is $0.024\text{cm}^3/\text{s}$ with the combination of the table speed and depth of cut is 20m/s and $20\mu\text{m}$ respectively. For single pass grinding, using 0.15% volume concentration zinc oxide nanocoolant, the minimum material removal rate is $0.020\text{cm}^3/\text{s}$ with the combination of the table speed and depth of cut is 20m/s and $20\mu\text{m}$ respectively. On the other hand, the maximum value is $0.155\text{cm}^3/\text{s}$ for 5% volume concentration of conventional coolant and $0.122\text{cm}^3/\text{s}$ for 0.15% volume concentration zinc oxide nanocoolant both at combination of the table speed and depth of cut is 20m/s and $60\mu\text{m}$ respectively.

Table 4.1: Material removal rate for each coolant and type of grinding

SPECIMEN	TABLE SPEED (m/s)	DEPTH OF CUT (μm)	MATERIAL REMOVAL RATE (cm^3/s)			
			SINGLE PASS		MULTIPLE PASS	
			Conventional Coolant	Nano Coolant	Conventional Coolant	Nano Coolant
A	20	20	0.024	0.020	0.032	0.023
B	20	40	0.049	0.041	0.056	0.045
C	20	60	0.072	0.061	0.081	0.071
D	30	20	0.031	0.025	0.041	0.031
E	30	40	0.065	0.053	0.073	0.063
F	30	60	0.096	0.081	0.105	0.093
G	40	20	0.045	0.037	0.063	0.046
H	40	40	0.096	0.079	0.112	0.095
I	40	60	0.155	0.122	0.159	0.156

There are slightly different in multiple pass grinding the minimum material removal rate in multiple pass grinding using 5% volume concentration of conventional coolant is $0.032\text{cm}^3/\text{s}$ with the combination of the table speed and depth of cut is 20m/s and $20\mu\text{m}$ respectively. For multiple pass grinding, using 0.15% volume concentration zinc oxide nanocoolant, the minimum material removal rate different is $0.023\text{cm}^3/\text{s}$ with the combination of the table speed and depth of cut is 40m/s and $20\mu\text{m}$ respectively. On the other hand, the maximum value is $0.159\text{cm}^3/\text{s}$ for 5% volume concentration of

conventional coolant and $0.156\text{cm}^3/\text{s}$ for 0.15% volume concentration zinc oxide nanocoolant both at combination of the table speed and depth of cut is 40m/s and $60\mu\text{m}$ respectively.

Figure 4.1 shows the various MRR value affect from various combinations of all factors, which is table speed, depth of cut, type of grinding and type of coolant. There are different in MRR value between single pass grinding and multiple pass grinding. Multiple pass grinding has higher MRR compare to the single pass. This is due to the in single pass, the grinding wheel only pass the specimen once. On the other hand, for multiple pass grinding, the grinding wheel pass 10 times. Therefore, the removal process occurs 10 times compare to single pass. However, there were also different between types of coolant, when using 0.15% volume concentration zinc oxide nanocoolant, the MRR slightly lower than MRR value when using 5% volume concentration of conventional coolant is used. This is due to the effect of the nano-particle that lubricated the two surfaces that slide each other. This is supported by the finding from Wu et al. (2006) and their findings are nanoparticulate form has exceptional tribological properties, which can reduce friction under extreme pressure conditions. Analysis of variance for first order are performed to model and predict the material removal rate for single pass grinding and multiple pass grinding using 0.15% volume concentration zinc oxide nanocoolant are represented in Table 4.2.

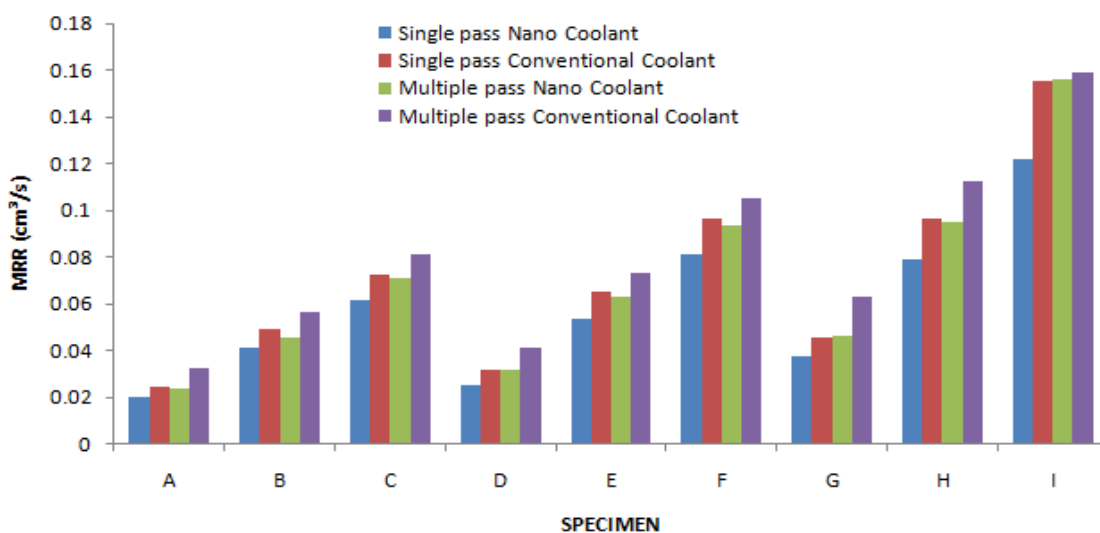


Figure 4.1: Material removal rate for each coolant and type of grinding

Table 4.2: ANOVA for first order MRR prediction in single pass and multiple pass grinding using 0.15% volume concentration zinc oxide water based nanocoolant

Source	Degree of freedom	Sum of sq.	F-static	P-value
Single pass grinding				
Model	3	0.00824733	98.4364	<.0001
Error	6	0.00016757		
C.Total	9	0.00841490		
Interaction	2			
Lack-of-Fit	5	0.00016307	7.2474	0.2745
Pure Error	1	0.00000450		
Total	6	0.00016757		
Multi-pass grinding				
Model	5	19.60468930	262.3551	<.0001
Error	4	0.14945158		
C.Total	9	19.75414088		
Interaction	2			
Lack-of-Fit	3	0.14878180	44.4271	0.1134
Pure Error	1	0.00066978		
Total	4	0.14945158		

The adequacy of the first-order model is verified using P-value of lack of fit. At a level of confidence of 95%, the models are checked for its adequacy. Based on ANOVA analysis, for the prediction of material removal rate (MRR) in both single pass grinding and multiple pass grinding process using 0.15% volume concentration zinc oxide water based nanocoolant in Table 4.2, the model are adequate due to the fact that the *P* values lack of fit are insignificant where is the value of 0.2745 for single pass grinding and 0.1134 for multiple pass grinding, which is larger than 0.05. This implies that the both model could fit, and it is adequate. Thus, the first order linear equation used to predict the material removal rate in single and multi-pass grinding process using 0.15% volume concentration zinc oxide water based nanocoolant could be express as Eq. (4.1) and Eq. (4.2) respectively:

$$MRR_{\text{First order single pass}} = 0.0569 + 0.01933x_1 + 0.03033x_2 + 0.011x_1x_2 \quad (4.1)$$

$$MRR_{\text{Fist order multipass}} = 0.3914 - 1.71845x_1 + 0.05564x_2 - 0.084825x_1x_2 \quad (4.2)$$

Even though the first-order model was found to be adequate, the second-order model was postulated to extend the variables range in obtaining the relationship between the MRR and the machining independent variables. The adequacy of the first-order model is verified using P-value of lack of fit. At a level of confidence of 95%, the models are checked for its adequacy. Based on ANOVA analysis, for the prediction of material removal rate (MRR) in both single pass and multiple pass grinding process using 0.15% volume concentration zinc oxide water based nanocoolant are presented in Table 4.3. The model is adequate due to the fact that the *P* values lack of fit is insignificant. The lack of fit value is 0.5504 for single pass grinding and 0.1313 for multiple pass grinding which is larger than 0.05. This implies that the both models are fit, and it is adequate.

Table 4.3: ANOVA for second order MRR prediction in single pass and multiple pass grinding using 0.15% volume concentration zinc oxide water based nanocoolant

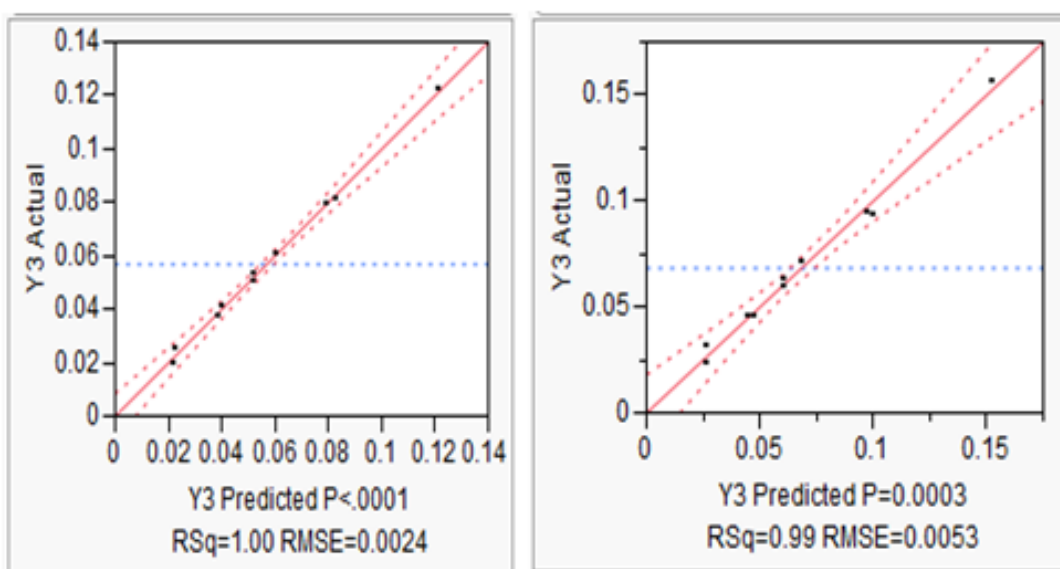
Source	Degree of freedom	Sum of sq.	F-static	P-value
Single pass grinding				
Model	5	0.00839245	291.6117	<.0001
Error	4	0.00002245		
C.Total	9	0.00841490		
Interaction	2			
Lack-of-Fit	3	0.00001795	1.3298	0.5504
Pure Error	1	0.00000450		
Total	4	0.00002245		
Multi-pass grinding				
Model	5	19.69133675	250.8286	<.0001
Error	4	0.06280412		
C.Total	9	19.75414088		
Interaction	2			
Lack-of-Fit	3	0.06213434	30.9228	0.1313
Pure Error	1	0.00066978		
Total	4	0.06280412		

The second order equation used to predict the MRR in single pass and multi pass grinding process for 0.15% volume concentration zinc oxide water based nano-coolant can be expressed as Eq. (4.3) and Eq. (4.4) respectively:

$$MRR_{2\text{ndorder}\text{singlepass}} = 0.05193 - 0.019333x_1 + 0.03033x_2 + 0.011x_1x_2 + 0.007643x_1^2 + 0.0006429x_2^2 \quad (4.3)$$

$$MRR_{2\text{ndorder}\text{multipass}} = 5.5109 - 1.7185x_1 + 0.5564x_2 - 0.08483x_1x_2 - 0.120473x_1^2 - 0.1282x_2^2 \quad (4.4)$$

Correlation studies are used to look for relationships between variables. There are three possible results of a correlation study: a positive correlation, a negative correlation, and no correlation. The correlation coefficient is a measure of correlation strength and can range from -1.00 to $+1.00$. Figure 4.2 shows the correlation between the second order models of MRR. It can be seen that there were no point outlier from the confident interval within 95%. The confident interval is cross the horizontal line beside make no asymptote with the horizontal line. This implies that the model could fit, and it is adequate with R-square equal to 1.00 and 0.99



(a) for single pass grinding

(b) for multiple pass grinding

Figure 4.2: Correlation of the second order model of MRR.

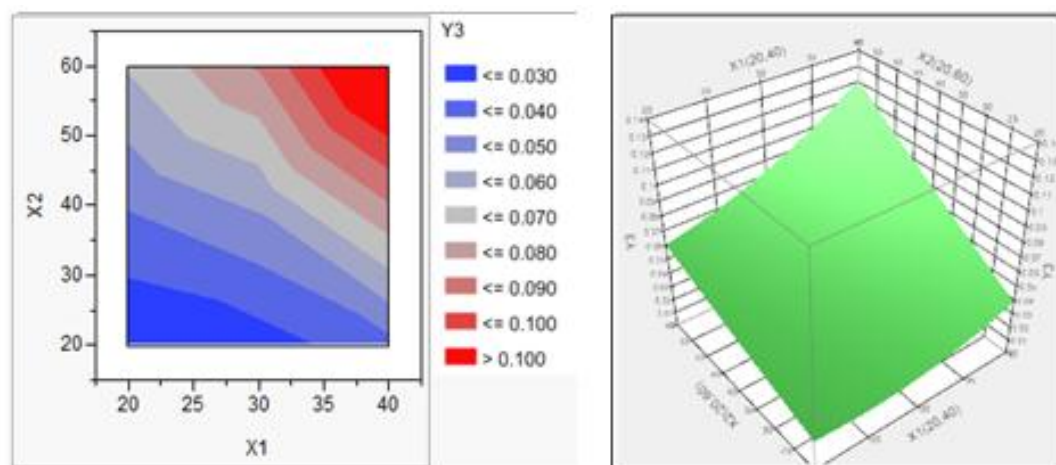
First and second-order models were constructed along with contour plots that more easily enable the selection of the proper combination of table speed and depth of cut to increase the material removal rate without sacrificing surface quality. Contour plot in Figure 4.3 are represented the relationship between depth of cut and table speed affect the MRR where x_1 represents table speed and depth of cut represented by x_2 . It observes maximum material removal rate both for single pass and multiple pass grinding is at depth of cut are maximum and table speed maximum. However, material removal rate is high in multiple pass grinding compare to single pass grinding. The MRR is highly sensitive to depth of cut. On the other hand, table speed has less effect on MRR. The MRR has a tendency to increase with increase in depth of cut and increase the table speed. When the depth of cut is low, the MRR is low sensitive to table speed. When the depth of cut is increase, it increases the MRR. However, this increasing becomes larger with the higher values table speed. It is also observed that the MRR variation pattern is identical for both single pass grinding and multiple pass grinding. In this study highlighted that depth of cut is major impact on material removal rate. Highest material removal rate could be produced when machined with a higher depth of cut, and highest table speed.

Table 4.4: Differentiate between experimental value and prediction value of MRR.

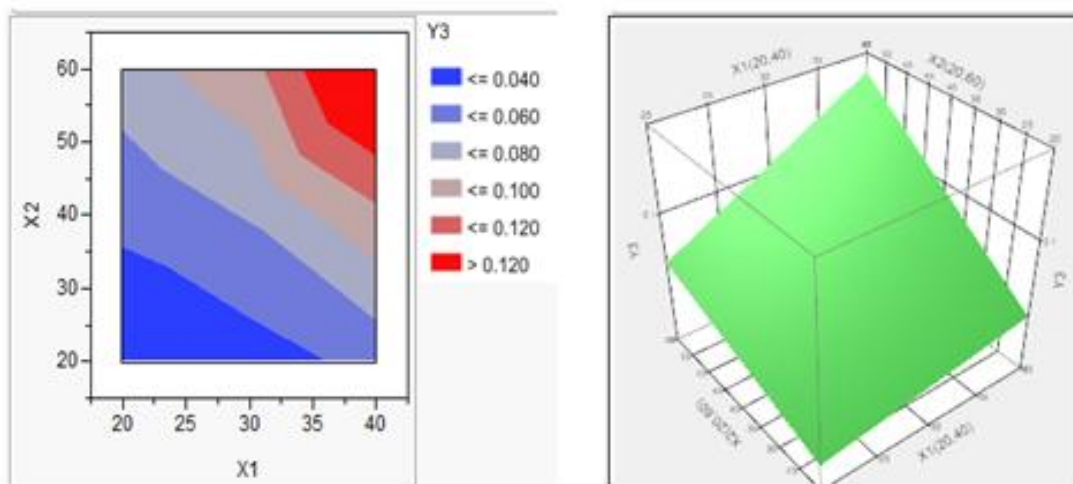
SPECIMEN	TABLE SPEED (m/s)	DEPTH OF CUT (μm)	MRR			
			Single pass grinding		Multiple pass grinding	
			Experimental Value	Prediction Value	Experimental Value	Prediction Value
A	20	20	0.020	0.018	0.023	0.021
B	20	40	0.041	0.038	0.045	0.042
C	20	60	0.061	0.057	0.071	0.063
D	30	20	0.025	0.027	0.031	0.032
E	30	40	0.053	0.057	0.063	0.068
F	30	60	0.081	0.087	0.093	0.105
G	40	20	0.037	0.035	0.046	0.042
H	40	40	0.079	0.076	0.095	0.095
I	40	60	0.122	0.118	0.156	0.147

To test the model is adequate and fit to predict the material removal rate in both single pass grinding and multiple pass grinding. The second order model was test by fit the model with value of depth of cut and table speed. Table 4.4 is listed the data for

experimental and predicted value of MRR model. Figure 4.4 illustrates the relationship between the experimental value and predicted value for both single pass grinding and multiple pass grinding. The predicted values and measured values are closely related, which indicated that the developed model could be effectively used to predict the MRR in the both grinding process even in multiple pass grinding as well as single pass grinding.



(a) for single pass grinding



(b) for multiple pass grinding

Figure 4.3: Contour plot of the second order model of MRR.

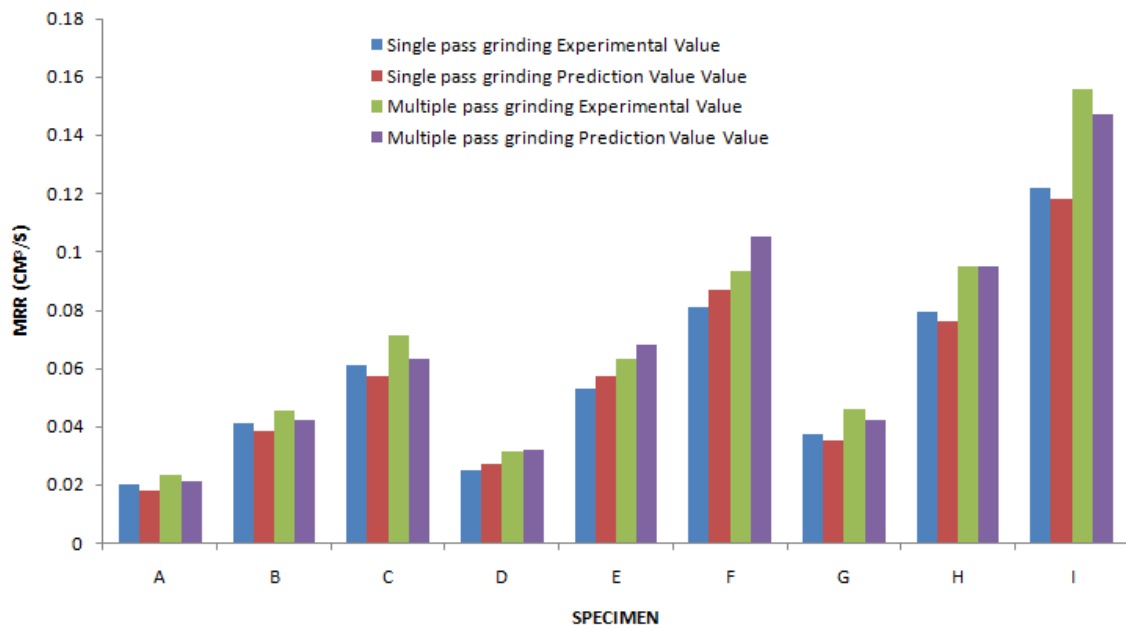


Figure 4.4: Relation between the experimental value and predicted value for both single pass grinding and multiple pass grinding.

4.3 TEMPERATURE EFFECT

Grinding is abrasive process, where the workpiece is force against the grinding wheel. Because of abrasive wear, the process generates chips that remove from the workpiece surface. However, the force that generate during the process are convert into heat that causes high temperature particularly at wheel and the workpiece interface in grinding process, high grinding zone temperature may lead to thermal damage to the work surface, induces micro-cracks and tensile residual stresses at the ground surfaces, which deteriorate surface quality and internality of the ground surface. This damage can reduced by the application of a flood delivery grinding fluid that removes the heat created by the workpiece interaction and lubricates the two surfaces in order to decrease the amount of friction. There are different in temperature rising between single pass and multiple pass grinding. From data observation single pass grinding generate low temperature rising due to the wheel only pass once time only compare to multiple pass that pass the workpiece 10 times. Heat are generate more during multiple pass and the force that generate during the process are convert into heat that will causing high temperature particularly at wheel and the workpiece interface. High temperatures can

cause thermal damage to the workpiece, which affects the workpiece quality and limits the process productivity (Malkin et al. 2007). Grinding wheel wear is also a major problem that needs to overcome. To control heat and wheel wear or to improve the grinding performance, a heavy amount of grinding fluids (coolant) is used.

Zinc oxide nanocoolant removes heat from grinding area efficiently compare to conventional this is due to high thermal conductivity of the nanocoolant enhanced from the water-based compare to the conventional coolant. Other reason why temperature rising low during grinding process using nanocoolant is, the nano-particle itself contribute to the tribological factor. It reduces the friction between the two surfaces that is grinding disk and specimen. From Table 4.5 shows the temperature rising for the single pass grinding. The first order and second order model was develop and analysis of variance are performed to model and predict the temperature rising for single pass grinding and multiple pass grinding using 0.15% volume concentration zinc oxide nanocoolant are represented in Table 4.6.

Table 4.5: Temperature rising.

Specimen	Table Speed (m/min)	Depth of Cut (μm)	TEMPERATURE RISING ($^{\circ}\text{C}$)			
			Single Pass		Multiple Pass	
			Conventional Coolant	Nano Coolant	Conventional Coolant	Nano Coolant
A	20	20	1	0	1	0
B	20	40	1	0	1	0
C	20	60	1	0	1	1
D	30	20	1	0	2	0
E	30	40	1	1	2	1
F	30	60	1	1	3	1
G	40	20	2	0	3	0
H	40	40	2	1	3	1
I	40	60	3	1	4	2

The adequacy of the first-order model is verified using P-value of lack of fit. At a level of confidence of 95%, the models are checked for its adequacy. Based on ANOVA analysis, for the prediction of temperature rising in both single pass grinding and multiple pass grinding process using 0.15% volume concentration zinc oxide water based nanocoolant in Table 4.6, the model are adequate due to the fact that the *P* values lack of fit are insignificant, which is the value is 0.2731 for single pass grinding and

0.3566 for multiple pass grinding. This implies that the both model could fit, and it is adequate.

Table 4.6: ANOVA for first order temperature prediction rising in single pass and multiple pass grinding using 0.15% volume concentration zinc oxide water based nanocoolant

Source	Degree of freedom	Sum of sq.	F-static	P-value
Single pass grinding				
Model	3	1.58333	4.2073	0.0637
Error	6	0.75267		
C.Total	9	2.33600		
Interaction	2			
Lack-of-Fit	5	0.73267	7.3267	0.2731
Pure Error	1	0.02000		
Total	6	0.75526		
Multi-pass grinding				
Model	3	3.58333	16.5639	0.0026
Error	6	0.43267		
C.Total	9	4.01600		
Interaction	2			
Lack-of-Fit	5	0.41267	4.1267	0.3566
Pure Error	1	0.02000		
Total	6			

First order linear equation for single pass and multiple pass grinding to predict the temperature rising in single pass grinding process using 0.15% volume concentration zinc oxide water based nanocoolant can be expressed as Eq. (4.5) and Eq. (4.6) respectively:

$$TR_{\text{First ordersinglepass}} = 0.48 + 0.333333x_1 + 0.333333x_2 + 0.25x_1 x_2 \quad (4.5)$$

$$TR_{\text{First ordermultiplepass}} = 0.68 + 0.333333x_1 + 0.66667x_2 + 0.25x_1 x_2 \quad (4.6)$$

Even though the first-order model was found to be adequate, the second-order model was postulated to extend the variables range in obtaining the relationship between the temperature rising and the machining independent variables. Based on ANOVA analysis, for the prediction of temperature rising in both single pass and multiple pass grinding process using 0.15% volume concentration zinc oxide water

based nanocoolant in Table 4.7, the model are adequate due to the fact that the P values lack of fit are not significant. Which is the value is 0.3963 for single pass grinding and 0.2730 for multiple pass grinding. Where is larger than 0.05. This implies that the both model could fit, and it is adequate.

Table 4.7: ANOVA for second order temperature rising in single pass and multiple pass grinding using 0.15% volume concentration zinc oxide water based nanocoolant

Source	Degree of freedom	Sum of sq.	F-static	P-value
Single pass grinding				
Model	5	0.1995	8.5663	0.0292
Error	4	2.3360		
C.Total	9	0.1995		
Interaction	2			
Lack-of-Fit	3	0.1795	2.9921	0.3963
Pure Error	1	0.0200		
Total	4	0.1995		
Multi-pass grinding				
Model	5	3.58790	6.74049	0.0445
Error	4	0.42809		
C.Total	9	4.01600		
Interaction	2			
Lack-of-Fit	3	0.40809	6.8016	0.2730
Pure Error	1	0.02000		
Total	4	0.42809		

The second order equation used to predict the temperature rising in single pass and multiple pass grinding process 0.15% volume concentration zinc oxide water based nanocoolant can be expressed as Eq. (4.7) and Eq. (4.8) respectively:

$$TR_{\text{Secondorder singlepass}} = 0.8572 + 0.33333x_1 + 0.33333x_2 + 0.25x_1x_2 - 0.3143x_1^2 - 0.3143x_2^2 \quad (4.7)$$

$$TR_{\text{Secondorder multiplepass}} = 0.71429 + 0.33333x_1 + 0.6667x_2 + 0.25x_1x_2 - 0.02857x_1^2 - 0.02857x_2^2 \quad (4.8)$$

Figure 4.5 presents the correlation between second order model of temperature rising for single pass and multiple pass grinding. There are no point outlier from the confident interval with was set to 95%. The confident interval is cross the horizontal line beside make no asymptote with the horizontal line. This implies that the model could fit, and it is adequate with R-square equal to 0.91 and 0.89.

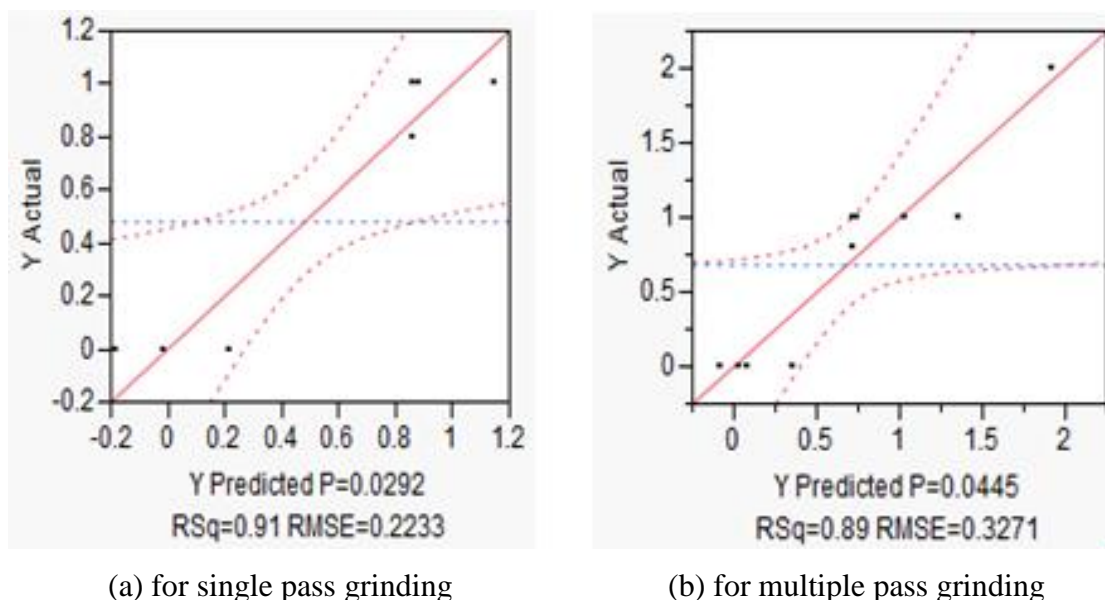
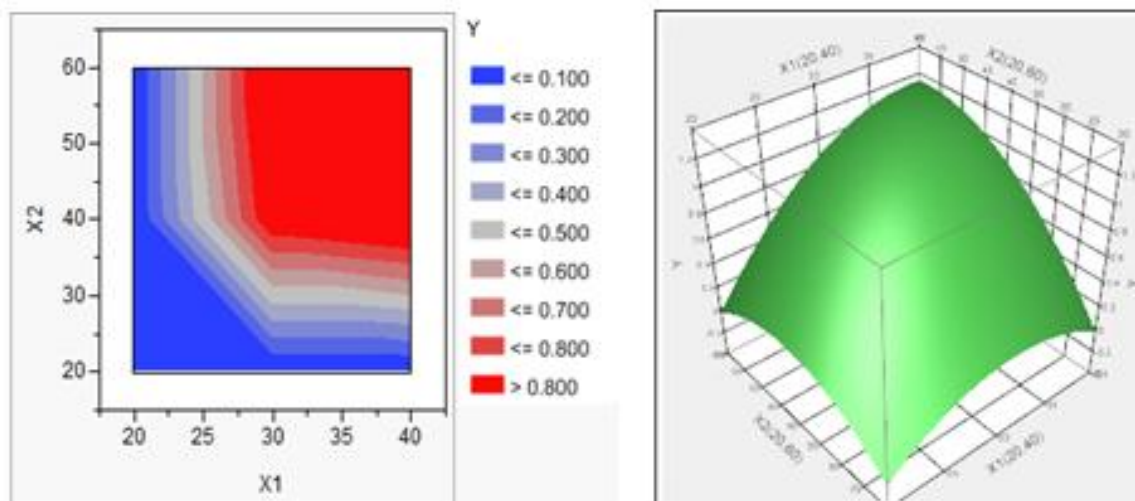


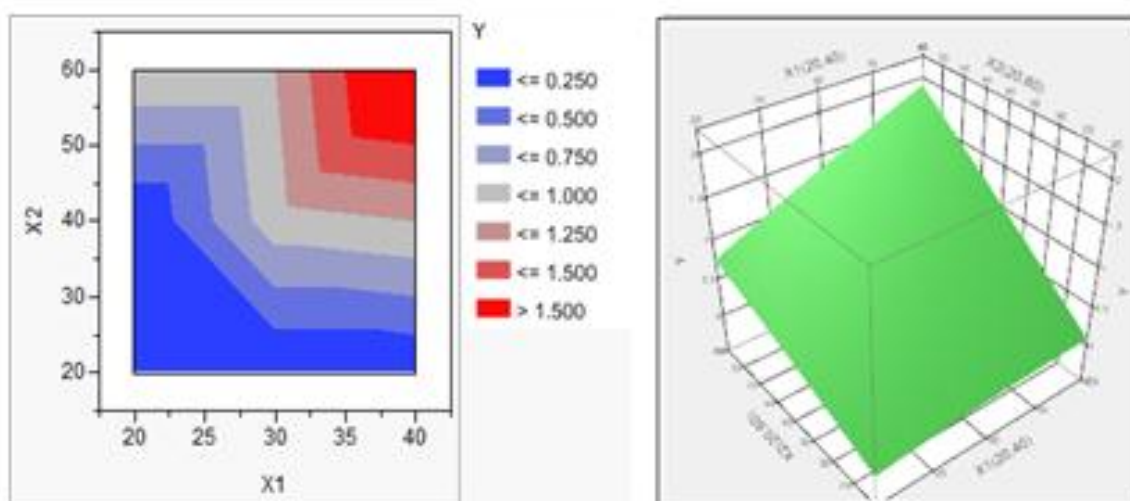
Figure 4.5: Correlation of the second order model of temperature rising.

First- order and second-order models were constructed along with contour plots that more easily enable the selection of the proper combination of table speed and depth of cut to decrease the temperature rising without sacrificing surface quality. Figure 4.6 shows the contour plot between depth of cut and table speed affect the temperature rising, where x_1 represents table speed and depth of cut represented by x_2 . It observes maximum temperature rising for single pass and multiple pass grinding at maximum depth of cut and table speed. However, temperature rising rate is high in multiple pass grinding compare to single pass grinding. The temperature rising is highly sensitive to depth of cut as well a stable speed. The temperature rising has a tendency to increase with increase in depth of cut and increase the table speed. When the depth of cut is low, the temperature rising is low sensitive to table speed. When depth of cut is increase, it increases the temperature rising. However, this increasing becomes larger with the higher values table speed. It is also observed that, the temperature rising variation

pattern is identical for both single pass grinding and multiple pass grinding. In this study highlighted that depth of cut is major impact on temperature rising. Highest temperature rising could be produced when machined with a higher depth of cut, and highest table speed and vice versa



(a) for single pass grinding



(b) for multiple pass grinding.

Figure 4.6: Contour plot (2D and 3D) of the second order model of temperature rising.

To test the model is adequate and fit to predict the material removal rate in both single pass grinding and multiple pass grinding. The second order model was test by fit the model with value of depth of cut and table speed. Table 4.8 shows the data for experimental value and predicted value from predicted MRR model. The predicted values and experimental values were much closed, which indicated that the developed model could be effectively used to predict the MRR in the both grinding process even in single pass grinding or multiple pass grinding. Figure 4.7 shows different between experimental values predicted value from predicted temperature rising model.

Table 4.8: Experimental and predicted value from predicted temperature rising model

SPECIMEN	TABLE SPEED (m/s)	DEPTH OF CUT (μm)	TEMPERATURE RISING			
			Single pass grinding		Multiple pass grinding	
			Experimental Value	Prediction Value	Experimental Value	Prediction Value
A	20	20	0	0.1882	0	0.09288
B	20	40	0	0.2094	0	0.35239
C	20	60	0	0.0216	1	0.74052
D	30	20	0	0.2094	0	0.01902
E	30	40	1	0.8570	1	0.71429
F	30	60	1	0.8760	1	1.35242
G	40	20	0	0.0216	0	0.07378
H	40	40	1	0.8760	1	1.01905
I	40	60	1	1.1450	2	1.90718

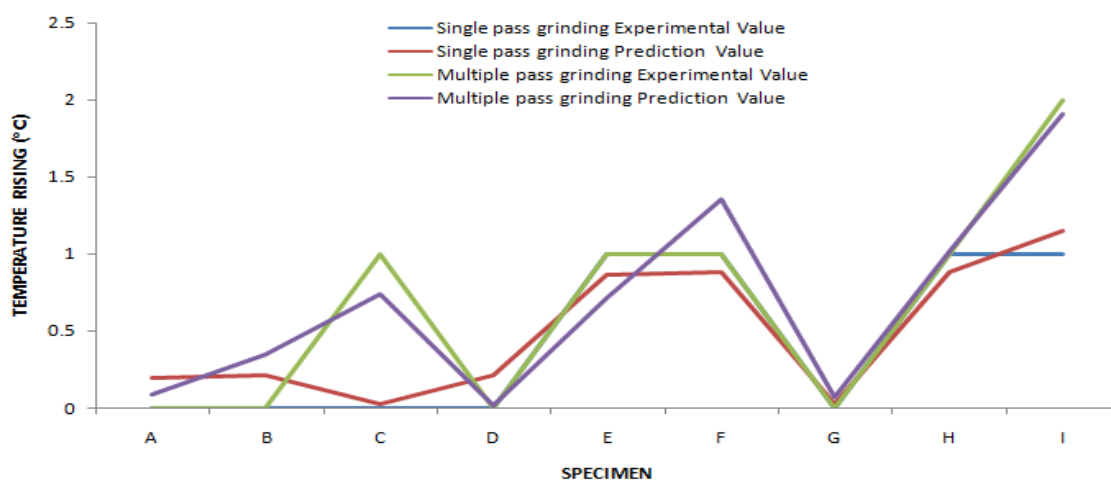


Figure 4.7: Different between experimental values predicted value from predicted temperature rising model.

4.4 SURFACE ROUGHNESS

Surface roughness is variable used for describe the quality of ground surface as well as competitiveness of overall grinding system as it determine the quality of the workpiece characteristic such as the minimum tolerance, the lubricant effectiveness, and the component life. The arithmetic average height parameter (R_a) is mostly used as an index to determine the surface finish in the machining process. It defines as Eq. (4.9):

$$R_a = \frac{1}{l} \int_0^l [y(x)] dx \quad (4.9)$$

Table 4.9 shows the tabulate data for surface roughness, three reading were taken, and average is calculated. The specimen was set on a flat surface and flat table before the perthometer take the reading. Before the reading taken the perthometer machine was calibrate first to ensure the precision. A good quality surface for most industrial application is with arithmetic mean roughness, R_a below $0.8\mu\text{m}$. The roughness average, R_a is the most used international parameter of surface roughness. It is defined surface roughness is the measure of the finer surface irregularities in the surface texture. It was quantified by the vertical deviations of a real surface from its ideal form. When these deviations are large, the surface is rough while they are small, therefore, the surface is smooth (Zhong and Venkatesh, 2008). A good quality surface for most industrial application is with arithmetic mean roughness, R_a below $0.8\mu\text{m}$. Type of grinding combine with type of coolant lead to good result where all the outcome or surface finish is less than $0.8\mu\text{m}$. First order and second order model was develop and analysis of variance are done to model and predict the material removal rate for single pass grinding and multiple pass grinding using 0.15% volume concentration zinc oxide nanocoolant are represented in Table 4.10.

The adequacy of the first-order model is verified using P-value of lack of fit. At a level of confidence of 95%, the models are checked for its adequacy. Based on ANOVA analysis, for the prediction of surface roughness in both single pass grinding and multiple pass grinding process using 0.15% volume concentration zinc oxide water based nanocoolant in Table 4.10, the model are adequate due to the fact that the P values lack of fit are insignificant. Which is the value is 0.0585 for single pass grinding

and 0.9920 for multiple pass grinding. Where is larger than 0.05. This implies that the both model could fit, and it is adequate.

Table 4.9: Surface finish for each coolant and type of grinding

Specimen	Table speed (m/min)	Depth of cut (μm)	SURFACE ROUGHNESS (Ra) / μm			
			Single Pass		Multiple Pass	
			Conventional coolant	Nano Coolant	Conventional coolant	Nano Coolant
A	20	20	0.321	0.415	0.276	0.359
B	20	40	0.265	0.253	0.226	0.353
C	20	60	0.241	0.551	0.291	0.324
D	30	20	0.181	0.340	0.189	0.172
E	30	40	0.151	0.306	0.224	0.237
F	30	60	0.286	0.508	0.186	0.229
G	40	20	0.237	0.374	0.233	0.294
H	40	40	0.304	0.492	0.316	0.322
I	40	60	0.489	0.546	0.401	0.507

Table 4.10: ANOVA for first order surface roughness prediction in single pass and multiple pass grinding using 0.15% volume concentration zinc oxide water based nanocoolant

Source	Degree of freedom	Sum of sq.	F-static	P-value
Single pass grinding				
Model	3	0.0443	1.4629	0.3158
Error	6	0.0605		
C.Total	9	0.1048		
Interaction	2			
Lack-of-Fit	5	0.0605	168.020	0.0585
Pure Error	1	0.000072		
Total	6	0.0606		
Multi-pass grinding				
Model	3	0.02584	0.8645	0.5090
Error	6	0.05939		
C.Total	9	0.08523		
Interaction	2			
Lack-of-Fit	5	0.05878	0.1806	0.9920
Pure Error	1	0.00061		
Total	6	0.05939		

First order linear equation used to predict the effect of surface roughness in single pass grinding and multiple pass grinding process using 0.15% volume

concentration zinc oxide water based nanocoolant can be expressed as Eq. (4.10) and Eq. (4.11) respectively:

$$SR_{\text{First order single pass}} = 0.4103 + 0.03216x_1 + 0.079333x_2 + 0.009x_1x_2 \quad (4.10)$$

$$SR_{\text{First order multiple pass}} = 0.2997 + 0.0145x_1 + 0.039167x_2 + 0.062x_1x_2 \quad (4.11)$$

Even though the first-order model was found to be adequate, the second-order model was postulated to extend the variables range in obtaining the relationship between the surface roughness and the machining independent variables. Based on ANOVA analysis, for the prediction of surface roughness in both single pass and multiple pass grinding process using 0.15% volume concentration zinc oxide water based nanocoolant in Table 4.11, the model are adequate due to the fact that the P values lack of fit insignificant which is the value is 0.071 for single pass grinding and 0.4499 for multiple pass grinding. This implies that the both model could fit, and it is adequate.

Table 4.11: ANOVA for second order surface roughness prediction in single pass and multiple pass grinding using 0.15% volume concentration zinc oxide water based nanocoolant

Source	Degree of freedom	Sum of sq.	F-static	P-value
Single pass grinding				
Model	5	0.08173886	2.8289	0.1677
Error	4	0.02311524		
C.Total	9	0.10485410		
Interaction	2			
Lack-of-Fit	3	0.02304324	106.68	0.071
Pure Error	1	0.00007200		
Total	4	0.02311524		
Multi-pass grinding				
Model	3	0.0803867	12.2695	0.0154
Error	6	0.0052414		
C.Total	9	0.0856281		
Interaction	2			
Lack-of-Fit	5	0.0045569	2.2191	0.4499
Pure Error	1	0.0006845		
Total	6	0.0052414		

The second order linear equation used to predict the surface roughness in single pass grinding and multiple pass grinding process 0.15% volume concentration zinc oxide water based nanocoolant can be expressed as Eq. (4.12) and Eq. (4.13):

$$SR_{\text{Secondorder singlepass}} = 0.3157 + 0.03216x_1 + 0.0793x_2 + 0.009x_1x_2 + 0.05307x_1^2 + 0.1046x_2^2 \quad (4.12)$$

$$SR_{\text{Secondorder multiplepass}} = 0.2045 + 0.00145x_1 + 0.039167x_2 + 0.062x_1x_2 + 0.148x_1^2 + 0.011x_2^2 \quad (4.13)$$

Figure 4.8 shows the correlation of the second model of surface roughness. From the confident interval with was set to 95%. In addition, the confident interval is cross the horizontal line beside make no asymptote with the horizontal line. This implies that the model could fit, and it is adequate with R-square equal to 0.78 and 0.94.

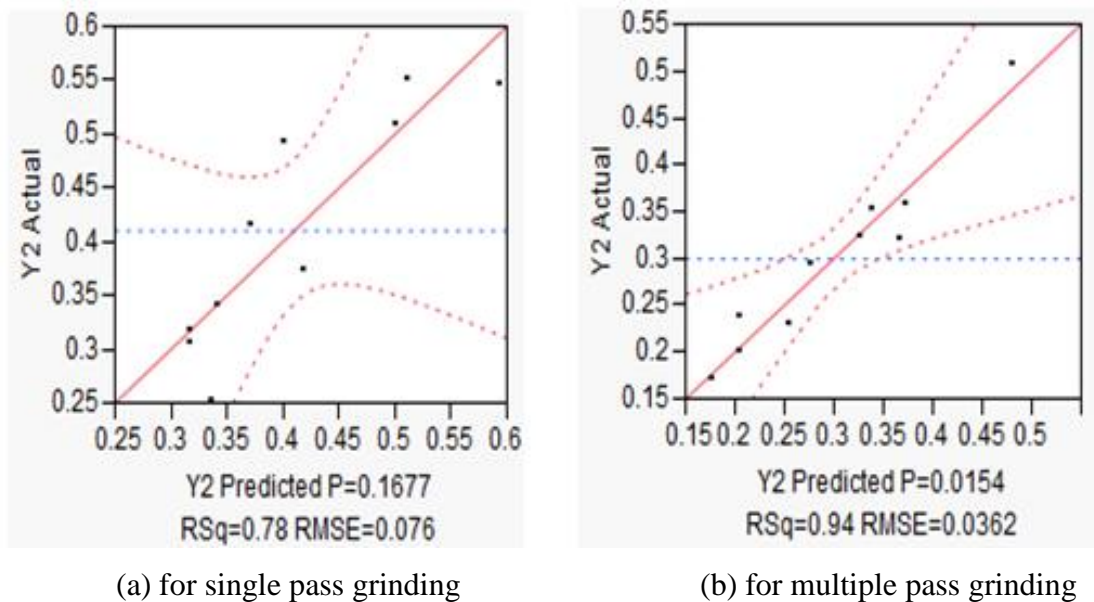


Figure 4.8: Correlation of the second order model of surface roughness

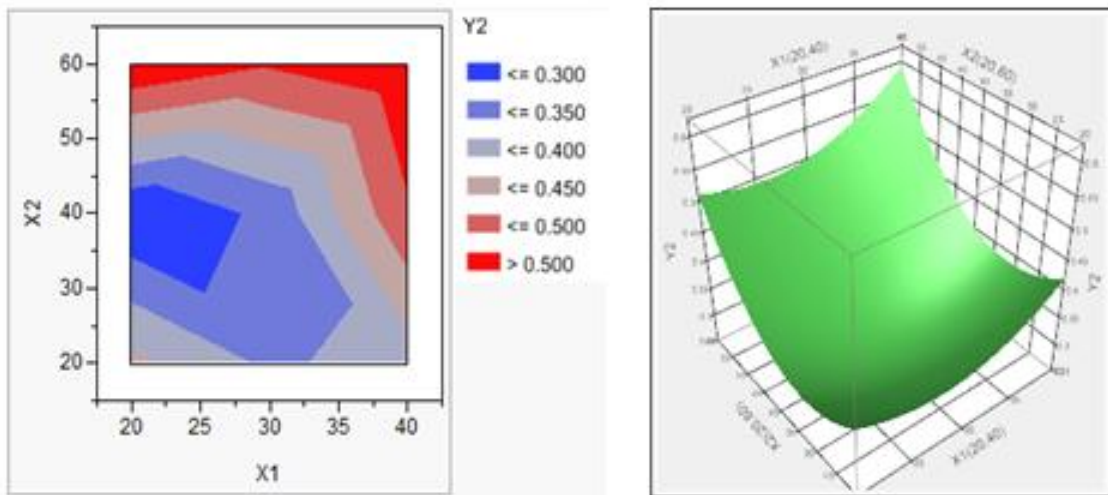
First- order and second-order models were constructed along with contour plots that more easily enable the selection of the proper combination of table speed and depth of cut to decrease the surface roughness. Contour plot in Figure 4.9 is represented the

relationship between depth of cut and table speed affect the temperature rising x_1 represents table speed and depth of cut represent by x_2 . It observes highest surface roughness both for single pass and multiple pass grinding is at depth of cut are maximum and table speed maximum. However, surface roughness is high in single pass grinding compare to multiple pass grinding. The surface roughness is highly sensitive to depth of cut as well a stable speed. The surface roughness has a tendency to increase with increase in depth of cut and increase the table speed. When the depth of cut is low, the surface roughness is low sensitive to table speed. When depth of cut is increase, it increases the surface roughness. However, this increasing becomes larger with the higher values table speed.

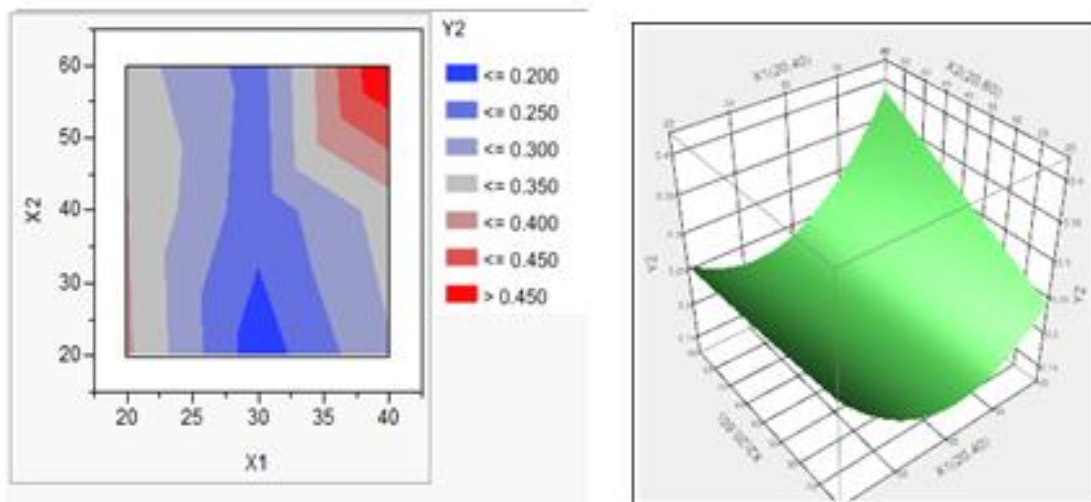
Table 4.12: Experimental and predicted value from predicted surface roughness model.

SPECIMEN	TABLE SPEED (m/s)	DEPTH OF CUT (μm)	SURFACE ROUGHNESS			
			Single pass grinding		Multiple pass grinding	
			Experimental Value	Prediction Value	Experimental Value	Prediction Value
A	20	20	0.415	0.3709	0.359	0.3498
B	20	40	0.253	0.3366	0.353	0.3380
C	20	60	0.551	0.5115	0.324	0.3041
D	30	20	0.340	0.3410	0.172	0.1543
E	30	40	0.306	0.3157	0.237	0.2045
F	30	60	0.508	0.4996	0.229	0.2326
G	40	20	0.374	0.4172	0.294	0.2548
H	40	40	0.415	0.3709	0.322	0.3670
I	40	60	0.253	0.3366	0.507	0.4571

To test the model is adequate and fit to predict the surface roughness in both single pass grinding and multiple pass grinding. The second order model was test by fit the model with value of depth of cut and table speed. Table 4.12 tabulates the data for experimental value and predicted value from predicted surface roughness model. The predicted values and measured values were close, which indicated that the developed model could be effectively used to predict the surface roughness in the both grinding process even in single pass grinding or multiple pass grinding. Figure 4.10 shows experimental and predicted value from predicted surface roughness model.



(a) for single pass grinding



(b) for multiple pass grinding

Figure 4.9: Contour plot of the second order model of surface roughness

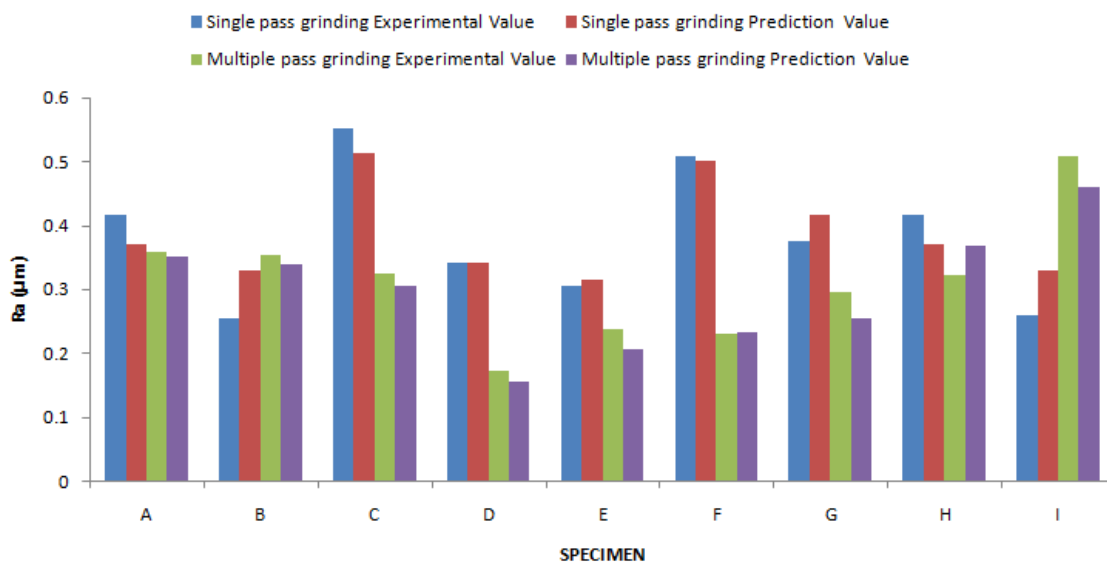


Figure 4.10: Experimental and predicted value from predicted surface roughness model.

4.5 TOOL WEAR

Tool wear is normal in machining process. However, there are many researches done to minimize this tool wear. Cutting tools are subjected to an extremely severe rubbing process. They are in metal-to-metal contact between the chip and workpiece, under conditions of very high stress at high temperature. The situation is further aggravated (worsened) due to the existence of extreme stress and temperature gradients near the surface of the tool. During machining, cutting tools remove material from the component to achieve the required shape, dimension and surface roughness (finish). However, wear occurs during the cutting action, and it will ultimately result in the failure of the cutting tool. When the tool wear reaches a certain extent, the tool or active edge has to be replaced to guarantee the desired cutting action. The tool wear was measured using vernier caliper. Several readings had taken and the average was calculated. Two readings were taken which are initial grinding disk width and final width. Initial grinding disk width taken before the grinding process started, and final width is width of the grinding disk after the grinding process had finished. The reading was taken at several points and the average was calculated. The tool wear is represented in Table 4.13.

From Table 4.13, the maximum wear in single pass grinding using conventional coolant is 0.2 cm occur in workpiece I, which have the most fast table speed and combine with highest value depth of cut. On the other hand, the minimum wear measured is 0.05cm occur in workpiece A, B and D and wear on the other setting of workpiece lying from 0.1 to 0.15 cm. For the maximum wear in single pass grinding using 0.15% volume concentration of zinc oxide nanocoolant, is 0.05cm which is occur in workpiece D,E,F,G,H and I. On the other hand, the minimum wear measured is 0.00cm or no wear detected, so it assume to be 0.01cm to make the variance analysis to be more converging, it occur in workpiece A,B and C. They are slightly different for multiple pass grinding, From the result that tabulate, the maximum wear in multiple pass grinding using conventional coolant is 0.45 cm which is occur in workpiece I, which have the most fast table speed and combine with highest value depth of cut. On the other hand, the minimum wear measured is 0.1cm occurs in workpiece B. Wear on the other setting of combination depth of cut and table speed, lying from 0.15 to 0.35cm. For the maximum wear in multiple pass grinding using 0.15% volume concentration of zinc oxide nanocoolant, is 0.2 cm which is occur in workpiece I. On the other hand, the minimum wear measured is 0.05cm it occur in workpiece A, B, C and D, wear on the other workpiece is lying from 0.1 to 0.15 cm.

Table 4.13: Tool wear for each coolant and type of grinding

Specimen	Table speed (m/min)	Depth of cut (μm)	TOOL WEAR (cm)			
			Single Pass		Multiple Pass	
			Conventional coolant	Nano Coolant	Conventional coolant	Nano Coolant
A	20	20	0.05	0.01	0.15	0.05
B	20	40	0.05	0.01	0.10	0.05
C	20	60	0.10	0.01	0.15	0.05
D	30	20	0.05	0.05	0.15	0.05
E	30	40	0.10	0.05	0.20	0.10
F	30	60	0.10	0.05	0.25	0.10
G	40	20	0.10	0.05	0.30	0.15
H	40	40	0.15	0.05	0.35	0.10
I	40	60	0.20	0.05	0.45	0.20

Figure 4.11 is a graph plotted to illustrate the tool wear for each 0.15% volume concentration of zinc oxide nanocoolant and 5% volume concentration water based soluble oil coolant respectively to type of grinding with combination of table speed and

depth of cut. In industrial tool wear should be minimized to have a good quality finish, precision and costing. From the graph plotted, for multiple pass the pattern of the wear plotted in increase as the depth of cut and table speed increase compared to the type of coolant, nanocoalant reduce the wear almost 50% compare to the conventional coolant. This is due to the nanocoalant reduce friction between the two contact surface.

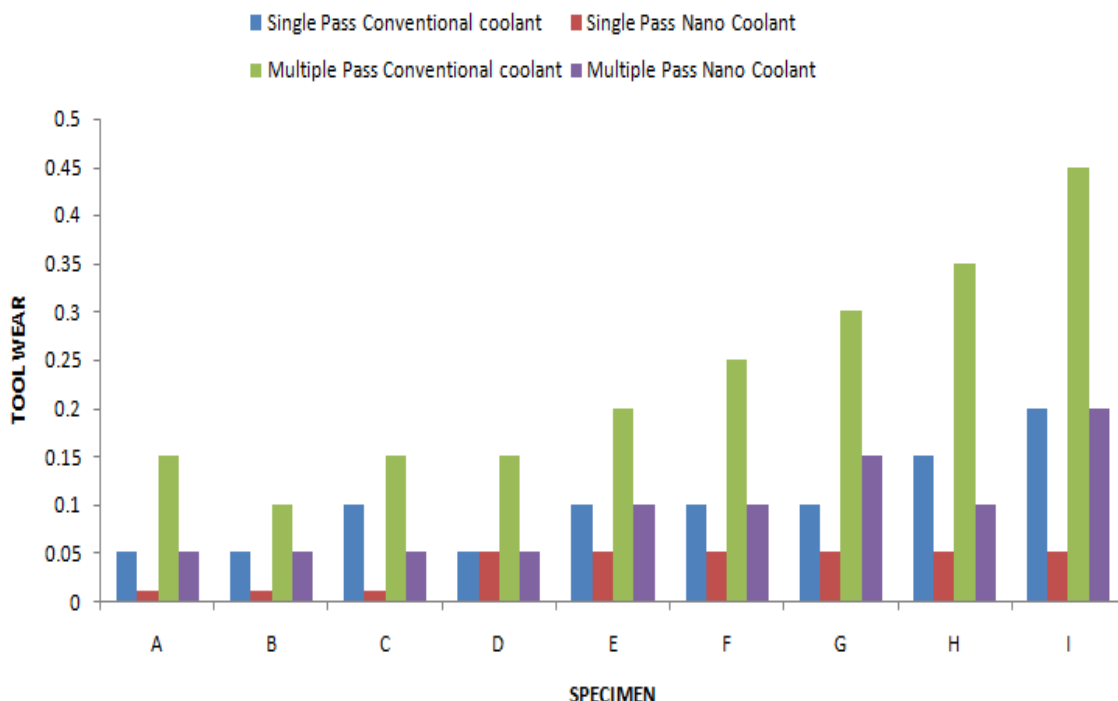


Figure 4.11: Tool wears each coolant and type of grinding

4.6 G-Ratio

G-ratio is element or parameter that interested to analyzed. The grinding wheel wear occurs due to the friction between the abrasive grains and the workpiece. High fluid lubricating capacity reduces the wear on the grinding wheel by decreasing grain-workpiece friction, allowing the abrasive grains to remain bound to the binder for longer periods and leading to lower wear of the tool (Silva et al.,2005). G-ratio is accepted parameter of wheel wear in the grinding ratio. It defines as Eq. (4.14):

$$G = \frac{\text{volume of material removed}}{\text{volume of wheel wear}} \quad (4.14)$$

As a result, the G-ratio should be maximized to have high value of material removal rate however at the same time the tool wear should be minimized. Table 4.14 listed the maximum G-ratio in single pass grinding using conventional coolant is 0.98 which is occur n workpiece B that have combination of 20m/s table speed and 40 μ m depth of cut. On the other hand, the minimum G-ratio is 0.45.

For the maximum wear in single pass grinding using 0.15% volume concentration of zinc oxide nanocoolant, is 6.10 which is occur in C. On the other hand, the minimum wear measured is 1.06 at setup workpiece E. They are slightly different for multiple pass grinding, From the result that tabulate, the maximum G-ratio in multiple pass grinding using conventional coolant is 0.54 which is occur in setup workpiece C. On the other hand, the minimum wear measured is 0.21 occurs in setup workpiece A and G.

For the maximum G-ratio in multiple pass grinding using 0.15% volume concentration of zinc oxide nanocoolant, is 1.42 which is occur in setup workpiece C. On the other hand, the minimum is measured is 0.31 it occur in workpiece G.

Table 4.14: G-ratio for each coolant and type of grinding

Specimen	Table Speed (m/s)	Depth Of Cut (μ m)	RATIO MRR TO TOOL WEAR			
			SINGLE PASS		MULTIPLE PASS	
			Conventional Coolant	Nano Coolant	Conventional Coolant	Nano Coolant
A	20	20	0.48	2.00	0.21	0.46
B	20	40	0.98	4.10	0.56	0.90
C	20	60	0.72	6.10	0.54	1.42
D	30	20	0.62	0.50	0.27	0.62
E	30	40	0.65	1.06	0.37	0.63
F	30	60	0.96	1.62	0.42	0.93
G	40	20	0.45	0.74	0.21	0.31
H	40	40	0.64	1.58	0.32	0.95
I	40	60	0.77	2.44	0.35	0.78

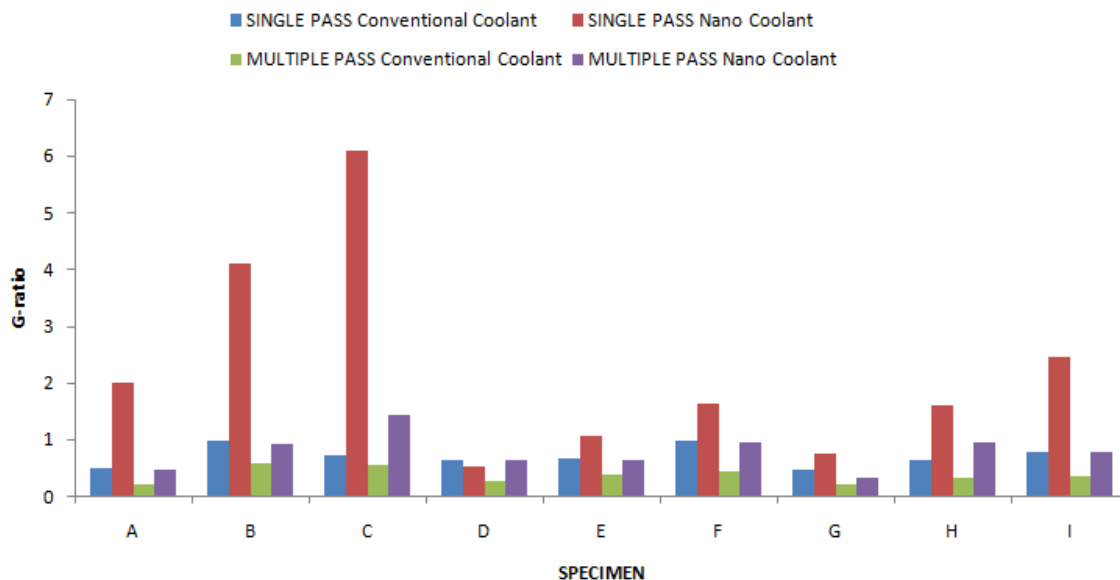


Figure 4.12: G-ratio for each coolant and type of grinding

Figure 4.12 illustrates the G-ratio for each coolant and type of grinding for each 0.15% volume concentration of zinc oxide nanocoolant and 5% volume concentration water based soluble oil coolant respectively to type of grinding with combination of table speed and depth of cut. In industrial G-ratio should be maximized to have a good quality finish, precision and costing. From the graph plotted, type of coolant influence the G-ratio as well as type of grinding, in single pass grinding the G-ratio are slightly high compare to the multiple pass grinding this is due in single pass grinding the grinding wheel only pass once so that the wear is minimized compare to the multiple passes that pass 10 times. Type of coolant is also given highest impact, lubricant from the nano-particle lead to maximize G-ratio compare to conventional coolant.

4.7 OPTIMIZATION

An optimization consists of maximizing or minimizing areal factor so that the output or the responses are in our desire. Generally, optimization is finding best available response from desire factor. Figure 4.13 shows prediction profiler for optimization in single pass grinding. It was set to have a minimize temperature rising (Y), minimize surface roughness (Y2), and maximize material removal rate (Y3). There for ethers is to have optimized value according to desirability, table speed net to set equal to 20mm/s and depth of cut 42.43 μ m. Thus, the output that come out from this

setting is 54.42% from desirability set earlier. According to model that generate the temperature rising minimize and predict to be 0.21°C , surface roughness is equal to $0.346\mu\text{m}$ and MRR is equal to $0.042597\text{cm}^3/\text{s}$ as illustrate by prediction profiler in Figure 4.13.

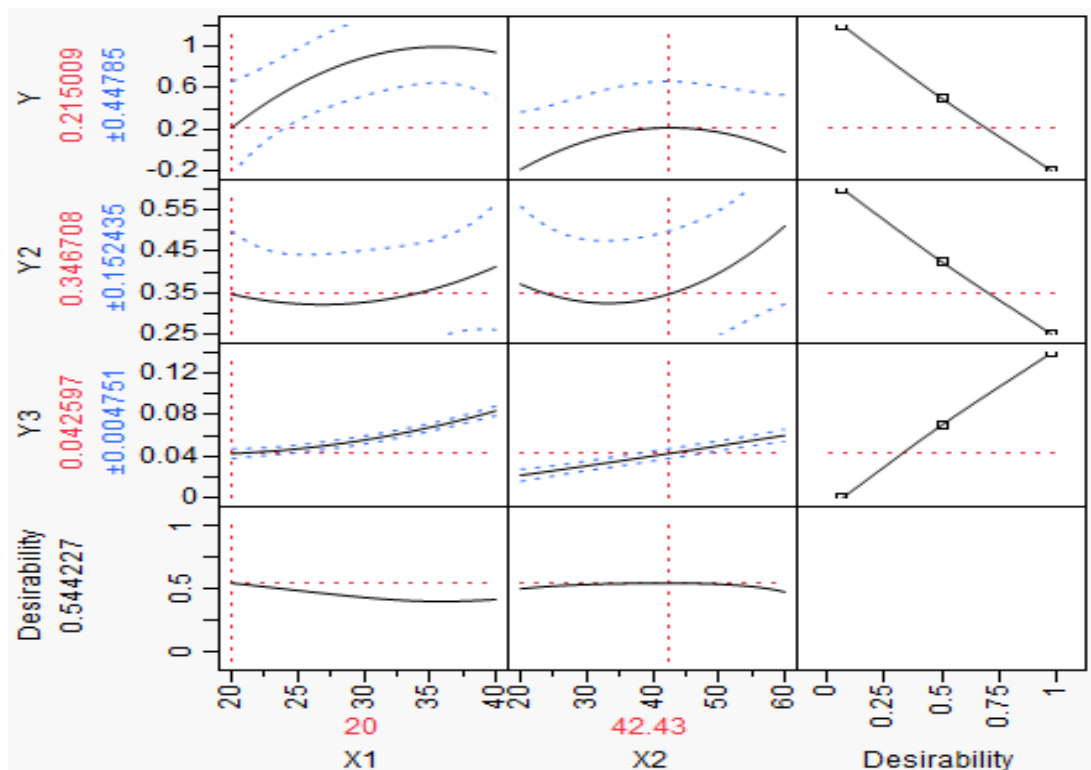


Figure 4.13: Prediction profiler for optimization in single pass grinding

Figure 4.14 presents prediction profiler for optimization in multiple pass grinding. Optimized value according to desirability, table speed net to set equal to 35.11mm/s and depth of cut $29.78\mu\text{m}$. Therefore, the output that come out from this setting is 57.69% from desirability set earlier. According to model that generate the temperature rising will minimize and predict to be 0.46°C , surface roughness is equal to $0.216\mu\text{m}$ and MRR is equal to $0.05467\text{cm}^3/\text{s}$. To have smooth surface roughness, type of grinding wheel and sized of grid of grinding wheel also affect the surface roughness. Small sized of grid performs better to have a good surface roughness.

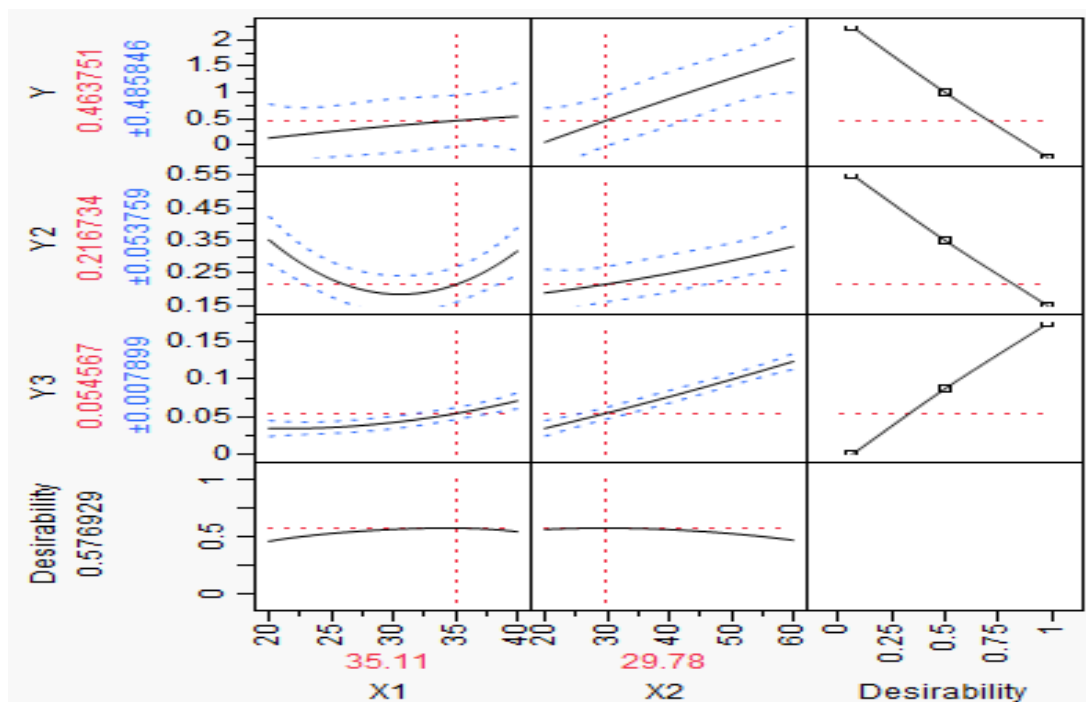


Figure 4.14.: Prediction profiler for optimization in multiple pass grinding

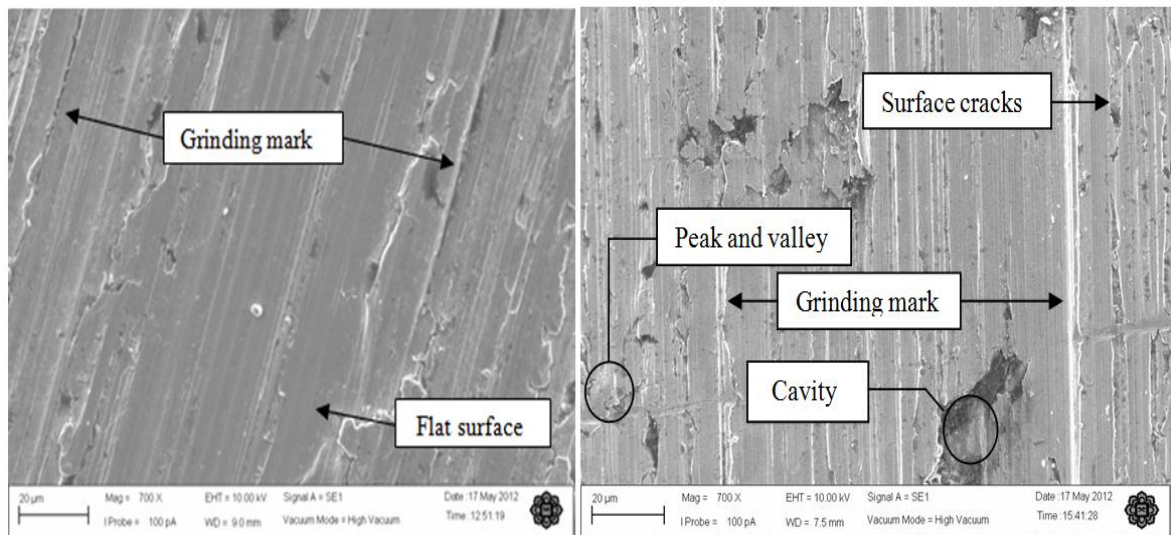
4.8 SCANNING ELECTRON MICROSCOPIC

The microscope is an extremely useful instrument in the examination of physical evidence. Most common is the optical microscope. With experience, a forensic microscopist can determine many specimens including glass, fibers, hair, paint chips, minerals, food particles, and more and can run small chemical identifications and spot tests. In this research for surface roughness analysis there are extra analysis had done where the specimen is undergo the scanning electron microscopic where it use a beam of electron to produce images with a magnification from 10x to 100,000x with greater depth of field than an optical microscope.

The surface of specimen I which undergo grinding process with maximum table speed equal to 40m/s and maximum depth of cut equal to 60 μ m was observe under 700 magnificent and represent in figure 4.15 represent the different of usage of both 5% volume concentration of nanocoolant and 0.15% volume concentration of zinc oxide nanocoolant. Figure 4.15(a) is surface of specimen I after grinding with applying of zinc oxide nanocoolant and figure 4.15(b) illustrate that surface of specimen I after grinding

with applying of conventional coolant. It clearly to make a conclusion that grinding using 0.15% volume concentration of zinc oxide will have better surface finish compare to 5% volume concentration of soluble oil water based coolant.

There are no cavity, peak and valley that will occur because of friction of the two sliding surface as well as surface crack which occur while heat density are too high while grinding process since zinc oxide nanocoolant will remove heat and decrease friction better compare to conventional coolant.



(a) for grinding using ZnO nanocoolant.

(b) for grinding using conventional coolant.

Figure 4.15: Scanning electron microscopic

CHAPTER 5

CONCLUSIONS AND RECOMMENDATIONS

5.1 CONCLUSIONS

The main objectives of this project are to investigate the performance of ductile cast iron during grinding process based on design of experiment and to develop mathematical model for abrasive machining parameter using response surface modeling using zinc oxide nanofluid as a coolant.

The performance of ductile cast iron during grinding process using 0.15% volume concentration of zinc oxide water based nanocoolant are in terms of temperature rising, application of 0.15% volume concentration of zinc oxide nanocoolant is more significant compare to 5% volume concentration water based soluble oil conventional coolant. This is due to nano-particle enhance the thermal conductivity of based fluid. High thermal conductivity leads to the high-heat transfer rate. Moreover, the tribological properties of nanocoolant leads to the low heat density generate since the friction between the two surfaces that slide each other are reduced.

In terms of tool wear, application of 0.15% volume concentration of zinc oxide nanocoolant is more significant compare to 5% volume concentration water based soluble oil conventional coolant. On the other hand, for material removal rate, application of 0.15% volume concentration of zinc oxide nanocoolant is insignificant compare to 5% volume concentration water based soluble oil conventional coolant. Both of them caused by the tribological properties of nanocoolant itself leading to the low wear since the friction between the two surfaces that slide each other are reduced. Nano-particle also loads to the grinding wheel; the uneven areas of the grinding wheel

are fulfilled by the nanoparticle itself and reduce the friction of the grinding wheel and workpiece. Less friction will be leading to low heat density generate and minimize the tool wear.

In terms of material removal rate, application of 0.15% volume concentration of zinc oxide nanocoolant is not significant compare to 5% volume concentration water based soluble oil conventional coolant. This is due to nano-particle the tribological properties of nanocoolant itself lead to the friction between the two surfaces that slide each other are reduced. However, it also affected the material removal rate (MRR), since nanofluid will reduce the friction between the grinding wheel and workpiece, the MRR also will reduce because of mass or volume of the workpiece remove is less compared to the conventional coolant.

Even though G-ratio does not depends on MRR. G-ratio should be maximized. The MRR should be maximized, and at the same time, the tool wear should be minimized due to surface finish, costing and quality. In terms of term of the tool G-ratio, application of 0.15% volume concentration of zinc oxide nanocoolant is more significant compare to 5% volume concentration water based soluble oil conventional coolant. This due to the tribological properties of nanocoolant itself leading to the low wear since the friction between the two surface that slide each other are reduced.

5.2 RECOMMENDATIONS FOR FUTURE WORK

The following recommendations are drawn based on present study.

- i) Future research can be conducted on formulation of new nanofluids to archive excellent tribological and thermal properties beside explore the feasibility industrial application such as in internal combustion engine, radiator etc.
- ii) Further research can be conducted on how different type of concentration of zinc oxide nanocoolant and effect of different type of grinding wheel beside effect of different coolant flow rate will affect the response that chosen.

REFERENCES

- Bang, I.C. and Kim, J.I.H. 2010. Thermal-fluid characterizations of ZnO and SiC nanofluids for advanced nuclear power plants. *Nuclear Technology*. **170**(1): 16-27.
- Bradley, N. 2007. *The response surface methodology*. Master Thesis, Indiana University of South Bend, Indiana, USA.
- Brinksmeier, E. and Minke, E. 1993. High-performance surface grinding- the influence of coolant on the abrasive process. *Annals of the CIRP*. **42**(1): 367–370.
- Cameron, A., Bauer, R. and Warkentin, A. 2010. an investigation of the effects of wheel-cleaning parameters in creep-feed grinding. *International Journal of Machine Tools and Manufacture*. **50**: 126-130.
- Chopkar, M., Das, P.K. and Manna, I. 2006. Synthesis and characterization of nanofluid for advanced heat transfer applications. *Scripta Materialia*. **55**(6): 549-552.
- Eastman, J.A., Choi, S.U.S., Li, S., Thompson, L.J. and Lee, S. 1997. Enhanced thermal conductivity through development of nanofluids. *Materials II*, ed. Komarnenl, S., Parker, J.C., Wollenberger, H.J. Pittsburgh: Materials Research Society.
- Gonzalez, B.H.K.D.H. and Mackay, D.J.C. 2001. Retained austenite in austempered ductile cast iron. *Material science and engineering*. **311**: 162-173
- Gopal, A.V. and Rao, P.V. 2003. Selection of optimum conditions for maximum material removal rate with surface finish and damage as constraints in SiC grinding, *International Journal of Machine Tools and Manufacture*. **43**: 1327-1336.
- Griffin, R.D., Li, H.J., Eleftheriou, E. and Bates, C.E. 2001. Machinability of gray cast iron, University of Alabama, Birmingham, Alabama.
- Guo, L., Xie, G. and Li, B. 2009. Grinding temperature in high speed deep grinding of engineering ceramics *International Journal of Abrasive Technology*. **2**(3): 245 - 258
- Han, Z.H., Cao, F.Y. and Yang, B. 2008. Synthesis and thermal characterization of phase changeable indium/polyalphaolefin nanofluids. *Applied Physics Letters*. **92**(24): 1-3.
- Hecker, R.L. and Liang, S.Y. 2003. Predictive modeling of surface roughness in grinding. *International Journal of Machine Tools & Manufacture*. **43**: 755-761.
- Hryniewicz, P., Szeri, A.Z. and Jahanmir, S. 2001. Application of lubrication theory to fluid flow in grinding: part 2—influence of wheel and surface roughness. *Journal of Tribology, ASME*. **123**(4): 101–107.

- Jang S.P. and Choi S.U.S. 2004. Role of Brownian motion in the enhanced thermal conductivity of nanofluid. *Applied Physics Letters*. **84**(21): 4316–4318.
- Kohli, S. P., Guo, C. and Malkin, S. 1995. Energy partition for grinding with aluminum oxide and CBN abrasive wheels. *Journal of Engineering for Industry*. **117**:160–168.
- Komanduri, R. and Reed, W.R. 1980. New technique of dressing and conditioning resin bonded superabrasive grinding wheels. *Annals of the CIRP*. **29**(1): 239– 243.
- Lee, S., Choi, S.U.S., Li, S. and Eastman, J.A. 1999. Measuring thermal conductivity of fluids containing oxide nanoparticles. *ASME Journal of Heat Transfer*. 121: 280-289
- Malkin, S. and Guo, C. 2007. Thermal analysis of grinding methodology: 1966-1988. *Technometrics*. **31**(2): 137-153.
- Montgomery, D.C. 2005. *Design and Analysis of Experiments: Response surface method and designs*. New Jersey: John Wiley and Sons, Inc.
- Murshed, S.M.S., Tan, S.H. and Nguyen, N.T. 2008. Temperature dependence of interfacial properties and viscosity of nanofluids for droplet-based microfluidics. *Journal of Physics D*. **41**(8): 1-5.
- Myers, R.H., Khuri, A.I. and Carter, W.H. Jr. 1989. *Response surface*. New York: W.H. Freeman and Company.
- Oehlert, G.W. 2000. Design and analysis of experiments: *Response surface design*. **277**: 100-103.
- Ramesh, K., Huang, H. and Yin, L. 2004. Analytical and experimental investigation of coolant velocity in high speed grinding. *International Journal of Machine Tools and Manufacture*. **44**: 1069–1076.
- Sahin, Y. and Motorcu, A.R. 2005. Surface roughness model for machining mild steel with coated carbide tool. *Materials and Design*. **26**: 321-326.
- Shen, B., Malshe, A.P., Kalita, P., and Shih, A.J. 2008. Performance and behavior of novel MoS₂ nanoparticles based grinding fluids in minimum quantity lubrication grinding. *Transactions of NAMRI/SME*. **36**: 357-364.
- Silva, L.R., Bianchi, E.C., Catai, R.E., Fuisse, R.Y., França, T.V. and Aguiar, P.R. 2005. Study on the behavior of the minimum quantity lubricant – MQL technique under different lubricating and cooling conditions when grinding ABNT 4340 steel. *Journal of the Brazilian Society of Mechanical Science and Engineering*. **17**(2):193-198.

- Singh, D., Toutbort, J., Chen G., et al. 2006. Heavy vehicle systems optimization merit review and peer evaluation. Annual Report, Argonne National Laboratory, Department of Energy, Washington, USA.
- Upadhyaya, R.P., and Malkin, S. 2004. Thermal aspects of grinding with electroplated CBN wheels. *ASME J. Manuf. Sci. Eng.* **126**: 107-114.
- Vajjha, R.S. and Das, D.K. 2009. Experimental determination of thermal conductivity of three nanofluids and development of new correlations. *International Journal of Heat and Mass Transfer.* **52**(21-22): 4675-4682.
- Verma, A., Jiang, W., Abu-Safe, H.H., and Malshe, A.P. 2008. Tribological behavior of the deagglomerated active inorganic nanoparticles for advanced lubrication. *Tribology Transactions.* **51**(5): 673-678.
- Wagener, M. and Gunther, B. 1999. Sputtering in liquids: a versatile process for the production of magnetic suspensions. *Journal of Magnetism and Magnetic Material.* **201**(4): 41-44
- Wang, X., Xu, X. and Choi, S.U.S. 1999. Thermal conductivity of nanoparticle-fluid mixture. *J. Thermophys. Heat Transfer.* **13**(4): 474-480.
- Wong, K.F.V. and Kurma. T. 2008. Transport properties of alumina nanofluids. *Nanotechnology.* **19**(34): 345702
- Wu, J.H., Phillips, B.S., Jiang, W., Sanders, J.H., Zabinski, J.S. and Malshe, A.P. 2006. Bio-inspired surface engineering and tribology of MoS₂ overcoated CBN-TiN composite coating. *Wear.* **261**: 592-599.
- Wyant, J.C. 1985. Measurement of roughness of supersmooth optical surfaces. *ACTA Polytech. Scand., Proc. Image Science '85, Helsinki, Finland Ph 150*, pp. 241-244.
- Xu, T., Zhang, J., and Xu, K. 1996. The ball-bearing effect of diamond nanoparticles as an oil additive. *Applied Physics.* **29**: 2932-2937.
- Yatsuya, S., Tsukasaki, Y., Mihama, K. and Uyeda, R. 1978. Preparation of extremely fine particles by vacuum evaporation onto a running oil substrate. *J. Cryst. Growth.* **45**: 490-494.
- Yu, W., France, D.M., Routbort, J.L. and Choi, S.U.S. 2008. Review and comparison of nanofluid thermal conductivity and heat transfer enhancements. *Heat Transfer Engineering.* **29**(5): 432-460.
- Zhong, Z.W. and Venkatesh, V.C. 2008. Recent developments in grinding of advanced materials. *Journal of Springer Link.* **8**: 1496-1503.

Zhu, H.T., Lin, Y.S. and Yin, Y.S. 2004. A novel one-step chemical method for preparation of copper nanofluids. *Journal of Colloid and Interface Science*. **277**:100–103

